Applied Energy 179 (2016) 17–35

Contents lists available at ScienceDirect

Applied Energy

journal homepage: www.elsevier.com/locate/apenergy

A mid-term, market-based power systems planning model

Nikolaos E. Koltsaklis [a,b,*], Athanasios S. Dagoumas [a], Michael C. Georgiadis [b], George Papaioannou [c], Christos Dikaiakos [c]

[a] University of Piraeus, School of Economics, Business and International Studies, Department of International and European Studies, PC 18532 Piraeus, Greece
[b] Aristotle University of Thessaloniki, Department of Chemical Engineering, 54124 Thessaloniki, Greece
[c] Independent Power Transmission System Operator S.A. (ADMIE), Department of Research, Technology and Development, PC 10443 Athens, Greece

HIGHLIGHTS

- A mid-term Energy Planning along with a Unit Commitment model is developed.
- The model identifies the optimum interconnection capacity.
- Electricity interconnections affect the power mix and the day-ahead spot price.
- Renewables' penetration has impacts on the power reserves and the CO_2 emissions.
- Energy policy and fuel pricing can have significant impacts on the power mix.

ARTICLE INFO

Article history:
Received 6 March 2016
Received in revised form 30 May 2016
Accepted 17 June 2016

Keywords:
Mixed integer linear programming
Unit commitment problem
Mid-term energy planning
Electric interconnections
Power markets

ABSTRACT

This paper presents a generic Mixed Integer Linear Programming (MILP) model that integrates a Mid-term Energy Planning (MEP) model, which implements generation and transmission system planning at a yearly level, with a Unit Commitment (UC) model, which performs the simulation of the Day-Ahead Electricity Market. The applicability of the proposed model is illustrated in a case study of the Greek interconnected power system. The aim is to evaluate a critical project in the Ten Year Network Development Plan (TYNDP) of the Independent Power Transmission System Operator S.A. (ADMIE), namely the electric interconnection of the Crete Island with the mainland electric system. The proposed modeling framework identifies the implementation (or not) of the interconnection of the Crete Island with the mainland electric system, as well as the optimum interconnection capacity. It also quantifies the effects on the Day-Ahead electricity market and on the energy mix. The paper demonstrates that the model can provide useful insights into the strategic and challenging decisions to be determined by investors and/or policy makers at a national and/or regional level, by providing the optimal energy road-map and management, as well as clear price signals on critical energy projects under real operating and design constraints.

1. Introduction

The integration of all European national electricity markets into a single one is of high priority on the political agenda of the European Commission. The security of the supply is one of the key drivers of the electricity market integration in Europe, as the implementation of interconnections among neighboring countries eliminate the effect of emergency situations. Integration of electricity markets can diversify the power generation mix, lower the electricity prices by creating more competitive and transparent markets, and give access to additional power generation capacity in case of a shortage in any one country [1]. Moreover, the expansion of grid interconnections is of utmost importance in order to facilitate the transition toward a power generation mix with very high levels of renewables penetration, by enabling full use of the flexibility of the power plants fleet and by increasing the flexibility to balance the variable wind output. [2–4]. Not surprisingly, the deployment of renewable energy at regions without extensive grid interconnections and far from the main load consuming centers could result in overloading of transmission lines [5].

The assessment of the value of the transmission capacity is a very complex task since it includes a large variety of issues such as power networks physics, power systems economics and reliability aspects. However, evolving supply and demand dynamics set a

* Corresponding author at: Aristotle University of Thessaloniki, Department of Chemical Engineering, 54124 Thessaloniki, Greece.
E-mail address: nikkoltsak@gmail.com (N.E. Koltsaklis).

http://dx.doi.org/10.1016/j.apenergy.2016.06.070
0306-2619/

Nomenclature

Acronyms

ADMIE	Independent Power Transmission System Operator S.A.
ETMEAR	special duty for the reduction of gas emissions
GAMS	General Algebraic Modeling System
LOLP	Loss of Load Probability
MEP	Mid-term Energy Planning
MILP	Mixed Integer Linear Programming
RAE	Regulatory Authority of Energy
RES	Renewable Energy Sources
SMP	system marginal price
TYNDP	Ten Year Network Development Plan

Sets

$(s,s') \in S$	set of subsystems
$(s,s') \in S^{IS}$	set of subsystems of the interconnected power system
$(s,s') \in S^{CR}$	set of subsystems of the autonomous power system
$(t,t') \in T$	set of hours
$e \in E$	set of pumped storage units
$b \in B$	set of blocks of the energy offer function (bids) of each hydrothermal and pumper storage unit as well as of each interconnection
$e \in E^s$	set of pumped storage units $e \in E$ interconnected with subsystem $s \in S$
$e \in E^z$	set of pumped storage units $e \in E$ interconnected with zone $z \in Z$
$f \in F$	set of transmission capacity range blocks between the mainland and the autonomous power system
$g \in G^h$	set of hydroelectric units
$g \in G^{hth}$	set of hydrothermal units
$g \in G^{res}$	set of renewable units (not including hydro units)
$g \in G^s$	set of units $g \in G$ that are installed in subsystem $s \in S$
$g \in G^{th}$	set of thermal units
$g \in G^z$	set of units $g \in G$ that are (or can be) installed in zone $z \in Z$
$g \in G$	set of all units
$m \in M$	set of months
$n \in N^s$	set of interconnected power systems $n \in N$ with subsystem $s \in S$
$n \in N^z$	set of interconnected power systems $n \in N$ with zone $z \in Z$
$n \in N$	set of interconnected power systems
$s \in S^{s'}$	set of subsystems $s \in S$ interconnected with subsystem $s' \neq s \in S$
$w \in W$	set of start-up types {hot, warm, cold}
$z \in Z$	set of zones

Parameters

$AF_{g,z,m,t}$	availability factor of each unit $g \in G^{res}$ in zone $z \in Z$, month $m \in M$ and hour $t \in T$ (p.u.)
$CB_{g,b,m,t}$	marginal cost of block $b \in B$ of the energy offer function of each unit $g \in G^{hth}$ in month $m \in M$ and hour $t \in T$ (€/MW)
$CEP_{n,b,m,t}$	marginal export bid of block $b \in B$ to interconnection $n \in N$ in month $m \in M$ and hour $t \in T$ (€/MW)
$CIP_{n,b,m,t}$	marginal cost of block $b \in B$ of the imported energy offer function from interconnection $n \in N$, in month $m \in M$ and hour $t \in T$ (€/MW)
CL_f	capacity range-f of the proposed interconnector between the mainland (interconnected) and the autonomous power system (MW)
$CPM_{e,b,m.t}$	marginal bid of block $b \in B$ of pumped storage unit $e \in E$ in month $m \in M$ and hour $t \in T$ (€/MW)
$D_{s,m,t}$	power load of subsystem $s \in S$, in month $m \in M$ and hour $t \in T$ (MW)
Dur_m	duration of each representative day of each month $m \in M$ (days)
$EP_{n,b,m,t}$	quantity of capacity block $b \in B$ of each energy export interconnection $n \in N$ in month $m \in M$ and hour $t \in T$ (MW)
$FL_{s,s',m,t}$	upper bound of the flow from subsystem $s \in S$ to subsystem $s' \neq s \in S$ in month $m \in M$ and hour $t \in T$ (MW)
$FR2^{down}_{m,t}$	system requirements in fast secondary-down reserve in month $m \in M$ and hour $t \in T$ (MW)
$FR2^{up}_{m,t}$	system requirements in fast secondary-up reserve in month $m \in M$ and hour $t \in T$ (MW)
IC^{int}_{res}	installed capacity of renewables in the mainland (interconnected) power system (MW)
IC^{tot}_{res}	installed capacity of renewables in both the mainland (interconnected) and autonomous power systems (MW)
INV_f	investment cost of transmission capacity block $f \in F$ (€/MW)
$IP_{n,b,m,t}$	quantity of capacity block $b \in B$ of each power imports interconnection $n \in N$ in month $m \in M$ and hour $t \in T$ (MW)
$L_{z,m,t}$	injection losses coefficient in zone $z \in Z$, month $m \in M$ and hour $t \in T$ (p.u.)
$NP_{g,m,t}$	fixed (non-priced) component of the energy offer function of each unit $g \in G$ in month $m \in M$ and hour $t \in T$ (MW)
$PCB_{g,b,m,t}$	power capacity block $b \in B$ of the energy offer function of unit $g \in G^{hth}$ in month $m \in M$ and hour $t \in T$ (MW)
$PC_{g,m,t}$	available power capacity of unit $g \in G$ in month $m \in M$ and hour $t \in T$ (MW)
$PMB_{e,b,m,t}$	quantity of capacity block $b \in B$ of pumped storage unit $e \in E$ in month $m \in M$ and hour $t \in T$ (MW)
$P^{max,sc}_g$	maximum power output (when providing secondary reserve) of each unit $g \in G^{hth}$ (MW)
P^{max}_g	maximum power output (dispatchable phase) of each unit $g \in G^{hth}$ (MW)
$P^{min,sc}_g$	minimum power output (when providing secondary reserve) of each unit $g \in G^{hth}$ (MW)
P^{min}_g	minimum power output (dispatchable phase) of each unit $g \in G^{hth}$ (MW)
P^{soak}_g	power output of each unit $g \in G^{hth}$ when operating in soak phase (MW)
$R1_g$	maximum contribution of unit $g \in G^{hth}$ in primary reserve (MW)
$R1^{up}_{m,t}$	system requirements in primary-up reserve in month $m \in M$ and hour $t \in T$ (MW)
$R2_g$	maximum contribution of unit $g \in G^{hth}$ in secondary reserve (MW)
$R2^{down}_{m,t}$	system requirements in secondary-down reserve in month $m \in M$ and hour $t \in T$ (MW)
$R2^{up}_{m,t}$	system requirements in secondary-up reserve in month $m \in M$ and hour $t \in T$ (MW)
$R3^{nsp}_g$	maximum contribution of unit $g \in G^{hth}$ in non-spinning tertiary reserve (MW)
$R3^{sp}_g$	maximum contribution of unit $g \in G^{hth}$ in spinning tertiary reserve (MW)
$R3_{m,t}$	system requirements in tertiary reserve in month $m \in M$ and hour $t \in T$ (MW)
$RC1_{g,m,t}$	price of the primary energy offer of each unit $g \in G^{hth}$, in month $m \in M$ and hour $t \in T$ (€/MW)
$RC2_{g,m,t}$	price of the secondary range energy offer of each unit $g \in G^{hth}$, in month $m \in M$ and hour $t \in T$ (€/MW)
R^{down}_g	ramp-down rate of unit $g \in G^{hth}$ (MW)

R_g^{sc} ramp rate (up and down) of unit $g \in G^{hth}$ when providing secondary reserve (MW)
R_g^{up} ramp-up rate of unit $g \in G^{hth}$ (MW)
SDC_g shut-down cost of each unit $g \in G^{hth}$ (€)
T_g^{htw} non-operational time of unit $g \in G^{hth}$ before going from hot to warm standby condition (h)
T_g^{desyn} desynchronization time of unit $g \in G^{hth}$ (h)
T_g^{down} minimum down time of unit $g \in G^{hth}$ (h)
T_g^{past} extended time period in the past (greater than the higher cold reservation time of all thermal units) (h)
T_g^{rdn} non-operational time (after being shut-down) of unit $g \in G^{hth}$ (h)
$T_g^{soak,w}$ type-w soak time of unit $g \in G^{hth}$ (h)
$T_g^{sync,w}$ type-w synchronization time of unit $g \in G^{hth}$ (h)
T_g^{up} minimum up time of unit $g \in G^{hth}$ (h)
T_g^{wtc} non-operational time of unit $g \in G^{hth}$ before going from warm to cold standby condition (h)

Continuous variables

$cfl_{s,s',f}$ capacity of the interconnector between the mainland (interconnected) and the autonomous power system whose bounds are in the determined capacity range-f (MW)
$exb_{n,b,m,t}$ cleared quantity of power capacity block $b \in B$ exported to interconnected system $n \in N$ in month $m \in M$ and hour $t \in T$ (MW)
$ex_{n,m,t}$ total energy withdrawal (exports) to interconnected system $n \in N$ in month $m \in M$ and hour $t \in T$ (MW)
$fr2_{g,m,t}^{down}$ contribution of unit $g \in G^{hth}$ in fast secondary-down reserve in month $m \in M$ and hour $t \in T$ (MW)
$fr2_{g,m,t}^{up}$ contribution of unit $g \in G^{hth}$ in fast secondary-up reserve in month $m \in M$ and hour $t \in T$ (MW)
$f_{s,s',m,t}$ corridor power flow from subsystem $s \in S$ to $s \neq s' \in S$ in month $m \in M$ and hour $t \in T$ (MW)
$imb_{n,b,m,t}$ cleared quantity of power capacity block $b \in B$ imported from interconnected system $n \in N$ in month $m \in M$ and hour $t \in T$ (MW)
$im_{n,m,t}$ total energy injection (imports) from interconnected system $n \in N$ in month $m \in M$ and hour $t \in T$ (MW)
$im_{n,m,t}^{net}$ net energy injection (imports) from interconnected system $n \in N$ in month $m \in M$ and hour $t \in T$ (MW)
$pb_{g,b,m,t}$ quantity of power capacity block $b \in B$ of unit $g \in G^{hth}$, dispatched in month $m \in M$ and hour $t \in T$ (MW)
$p_{g,m,t}$ energy injection (generation) from unit $g \in G^{hth}$ in month $m \in M$ and hour $t \in T$ (MW)
$p_{g,m,t}^{desyn}$ power output of unit $g \in G^{hth}$ when operating in the desynchronization phase in month $m \in M$ and hour $t \in T$ (MW)
$p_{g,m,t}^{net}$ net energy injection from unit $g \in G^{hth}$ in month $m \in M$ and hour $t \in T$ (MW)
$p_{g,m,t}^{soak}$ power output of unit $g \in G^{hth}$ when operating in the soak phase in month $m \in M$ and hour $t \in T$ (MW)
$pmb_{e,b,m,t}^{pum}$ cleared quantity of block $b \in B$ of pumping unit $e \in E$ in month $m \in M$ and hour $t \in T$ (MW)
$pm_{e,m,t}^{pum}$ total cleared quantity of pumping unit $e \in E$ in month $m \in M$ and hour $t \in T$ (MW)
$r1_{g,m,t}^{up}$ contribution of unit $g \in G^{hth}$ in primary-up reserve in month $m \in M$ and hour $t \in T$ (MW)
$r2_{g,m,t}^{down}$ contribution of unit $g \in G^{hth}$ in secondary-down reserve in month $m \in M$ and hour $t \in T$ (MW)
$r2_{g,m,t}^{up}$ contribution of unit $g \in G^{hth}$ in secondary-up reserve in month $m \in M$ and hour $t \in T$ (MW)
$r3_{g,m,t}$ contribution of unit $g \in G^{hth}$ in tertiary reserve in month $m \in M$ and hour $t \in T$ (MW)
$r3_{g,m,t}^{nsp}$ contribution of unit $g \in G^{hth}$ in non-spinning tertiary reserve in month $m \in M$ and hour $t \in T$ (MW)
$r3_{g,m,t}^{sp}$ contribution of unit $g \in G^{hth}$ in spinning tertiary reserve in month $m \in M$ and hour $t \in T$ (MW)

Binary variables

$x_{g,m,t}$ 1, if unit $g \in G^{hth}$ is committed (operational) in month $m \in M$ and hour $t \in T$
$x_{g,m,t}^{3ns}$ 1, if unit $g \in G^{hth}$ contributes to non-spinning tertiary reserve in month $m \in M$ and hour $t \in T$
$x_{g,m,t}^{desyn}$ 1, if unit $g \in G^{hth}$ operates in the desynchronization phase in month $m \in M$ and hour $t \in T$
$x_{g,m,t}^{disp}$ 1, if unit $g \in G^{hth}$ operates in the dispatchable phase in month $m \in M$ and hour $t \in T$
$x_{g,m,t}^{sd}$ 1, if unit $g \in G^{hth}$ shut-downs in month $m \in M$ and hour $t \in T$
$x_{g,m,t}^{sec}$ 1, if unit $g \in G^{hth}$ contributes to secondary reserve in month $m \in M$ and hour $t \in T$
$x_{g,m,t}^{soak,w}$ 1, if unit $g \in G^{hth}$ operates in the type-w soak phase in month $m \in M$ and hour $t \in T$
$x_{g,m,t}^{soak}$ 1, if unit $g \in G^{hth}$ operates in the soak phase in month $m \in M$ and hour $t \in T$
$x_{g,m,t}^{st,w}$ 1, if a type-w start-up decision is taken for unit $g \in G^{hth}$ in month $m \in M$ and hour $t \in T$
$x_{g,m,t}^{st}$ 1, if unit $g \in G^{hth}$ starts-up in month $m \in M$ and hour $t \in T$
$x_{g,m,t}^{sync,w}$ 1, if unit $g \in G^{hth}$ operates in the type-w synchronization phase in month $m \in M$ and hour $t \in T$
$x_{g,m,t}^{sync}$ 1, if unit $g \in G^{hth}$ operates in the synchronization phase in month $m \in M$ and hour $t \in T$
y_f 1, if capacity range-f interconnector is to be installed between the mainland (interconnected) and the autonomous power system

new basis for investments in new transmission capacity, especially between grids with complementary characteristics. Pineau et al. [6] highlight the impacts that natural gas prices could have on the value of interconnectors, while climate change does not seem to significantly affect the projected revenues of transmission lines. Lienert and Lochner [7] investigated possible market interrelations between the European electricity and natural gas markets through an integrated linear programming mathematical model. Tande and Korpås [8] studied the combined effects of wind power and grid transmission capacity expansion on Loss of Load Probability (LOLP), and their findings suggest a positive correlation among these parameters and the system adequacy.

Lynch et al. [9] developed a mixed-integer linear programming (MILP) model for the determination of the optimal interconnection investments between jurisdictions for a certain level of renewable penetration. The findings suggest that new interconnections are in line with reduced generation capacity investments and total costs only when there is renewable penetration target. Denny et al. [10] made use of a stochastic unit commitment model to assess the influence of increased interconnection for the island of Ireland with high penetrations of wind generation. The findings indicate that increased interconnections can decrease average prices as well as their variability, while they can enhance power system security to a significant extent. Edmunds et al. [11] demonstrated that increased interconnections and energy storage capabilities could facilitate and lead to increased wind penetration and as a consequence, to reduced carbon emissions intensity. Chang and Li [12] developed a dynamic linear programming model and applied it to a set of multiple countries with cross-border electricity trading. The findings of their study highlight the significant cost savings

that can be achieved due to increased power trade among the selected countries, as well as the importance of the geographical location, which constitutes a key driver on where to construct new power generation capacity and to export power. One interesting observation is that hydropower appears to be fully utilized when large-scale electricity trading across the region is permitted and a more intense utilization of renewable energy occurs at high levels of electricity trading. Zafeiratou and Spataru [13] investigated the potential of significant renewable energy (wind and solar) penetration in the Greek island of Syros, which is to be interconnected with the mainland (interconnected power system). They also highlighted the benefits (e.g., energy security, exploitation of local energy resources, and elimination of oil use) as well as the challenges that have yet to be addressed.

In addition to interconnectors, demand response resources can also have noticeable impacts on the electricity markets' operation. Magnago et al. [14] found that demand response mechanisms have the potential to decrease electricity prices, causing significant diversifications on social welfare, in favor of the consumers.

Simoglou et al. [15] presented a scenario-based simulation analysis of the operation of the power system of the island of Crete, in order to evaluate the impact of high renewable energy penetration on the short-term power system scheduling. According to the authors, there is a potential for higher Renewable Energy Sources (RES) penetration levels accompanied with the utilization of a pumped-storage plant or another form of energy storage facility. This work does not consider the possibility of the island's interconnection with the mainland. Vidal-Amaro et al. [16] presented a methodology for assessing optimal energy mixes with high share of renewable energy. Pereira et al. [17] developed a multi-objective mixed integer linear programming model to address the generation expansion planning problem by integrating an increasing share of renewable energy in the power system. The authors made use of monthly load blocks in an attempt to capture the seasonality of the renewable resources.

Forrest and MacGill [18] employed econometric analysis techniques to evaluate the impact of wind power generation on electricity prices as well as on gas- and coal-fired generation. The results show a negative correlation between wind output and electricity price and that natural gas-fired power generation is mainly affected by increased wind output, while coal-fired power generation is less affected by that evolution. Clò et al. [19] made an analysis of the Italian wholesale power market and found that over the period 2005–2013, a rise of 1 GW h in the hourly average of daily wind and solar power generation has, on average, reduced wholesale electricity prices by respectively 2.3 €/MW h and 4.2 €/MW h and has made them more volatile. When each power generation technology, i.e., wind and solar, is examined individually, it has been found that the utilization of solar energy has led to a reduction in consumer surplus, while the opposite occurs in the case of wind energy (considering the levelized cost of energy and the cost of the supporting schemes of each technology).

Clancy et al. [20] evaluated for a specific power system in Ireland the avoided CO_2 emissions and the use of fossil fuels due to the presence of installed renewable power units. Zafirakis et al. [21] quantified the impact of cross-border power trade on national CO_2 emissions of European countries and studied the potential of preventing energy exports from countries with high CO_2 emissions intensity to others with low emissions intensity through the use of different levels of pumped hydro storage.

As far as the Greek power system is concerned, the interconnection of the islands and especially of the Crete Island, is the most important energy infrastructure development that the Independent Power Transmission System Operator S.A. (ADMIE) has undertaken to implement in its Ten Year Network Development Plan (TYNDP). The Regulatory Authority of Energy (RAE) has approved, through its 560/2013 decision, the TYNDP for the period 2014–2023, mentioning that ADMIE has to make a final decision – until the submission of the TYNDP for 2015–2024 – on the following critical issues concerning the Crete interconnection: identification of the interconnection nodes in the mainland and the Crete electric system, and identification of the dimension of the interconnection cable (e.g. 2 cables of 500 MW each). ADMIE is already elaborating its new TYNDP, trying to resolve those critical issues, which concern economic, technical and environmental issues, as the interconnection node – especially in the Crete Island – faces local opposition from municipalities and citizens [22]. Moreover the dimensioning of the cable strongly affects the installation of major renewables plants, as the wind and solar potential is exceptionally high, making wind investments competitive to conventional ones, such as lignite and gas power plants, as the levelized cost of electricity is lower for several wind investments. However, again there is local opposition for the construction of massive wind farms from the local societies. All these issues create uncertainties on the connection node, the size of the cable and the time of its implementation.

This work does not aim to contribute on resolving any of issues related to local concerns, especially environmental or other considerations. It aims at developing an appropriate model, following a literature review, that identifies the need for developing an integrated mid-term energy planning and unit commitment model which considers also critical elements of the system, such as the dimensioning of the interconnection cables, besides the available methodologies for electricity generation. The proposed model is able to quantify the effect of the interconnection of Crete in the electricity market of the mainland system, by determining the feasibility of its construction (and the corresponding capacity) or not. It also aims to provide its effect on the marginal system price of the Day-Ahead Electricity Market and on the energy mix, providing also evidence on the penetration capability of renewables.

The current work constitutes an integrated approach which combines a mid-term energy planning (at a single year level) with a unit commitment model (at an hourly level). This approach is based on our previous work [23], incorporating also the strategic decision-option for the interconnection with the mainland power system of a relatively large neighboring power system, which could be an autonomous domestic system such as the Crete Island, or a neighboring country. The key decisions to be determined by the model include: (i) optimal yearly energy mix, (ii) construction or not of the interconnector as well as its rated capacity, (iii) system's zonal marginal price values, and (iv) reserve provision allocation per technology type.

In order to quantify these effects, the Mid-term Energy Planning (MEP) problem, which identifies the units that will be commissioned and the dimensioning of critical network system elements, based on a mixed-integer optimization framework that considers techno-economic and environmental criteria, has to be integrated with the Unit Commitment (UC) problem. The latter identifies the units that will operate in the day-ahead electricity market based on an optimization approach that considers their variable costs, their bidding strategy, the ancillary services and other technical criteria required by the Transmission System Operator.

The key contributions and the salient features of our work include: (i) mid-term transmission expansion planning, (ii) market-based integration of independent power systems, (iii) quantification of the impacts of different penetration levels of renewables on the energy mix and on the reserve allocation, and (iv) integration between strategic investment decisions and daily generation scheduling.

The remainder of the paper is organized as follows: Section 2 presents the problem statement, while Section 3 provides the formulation of the model. Section 4 presents the details of a case study, while Section 4 provides an analytical discussion of the

results obtained for some indicative scenarios concerning the interconnection of Crete with the mainland Greek power system. Finally, Section 6 draws up the main conclusions arising from the implementation of this work.

2. Problem statement

The problem to be addressed in this work is concerned with the annual energy balance of a specific power system including the optimal dispatch of power generating units (operational part – unit commitment problem), while taking into account design decisions such as the possible interconnection with a neighboring power system, which could be an autonomous domestic system as the Crete Island, or a neighboring country (design part – transmissions expansion planning problem). The problem under consideration is formally defined in terms of the following items:

- The scheduling period includes hourly time steps $t \in T$, where the electricity market operator determines the optimal scheduling plan for the 24 h of the next day (day-ahead market). The design period is annual and this is achieved by incorporating twelve representative days (one per month) at an hourly time scale (24 h). The scheduling problem is integrated with the design problem and constitutes the extended annual energy balance problem to be solved. The duration of each representative day (in days) is given by Dur_m.
- The power system under consideration is split into a number of subsystems $s \in S$. These subsystems are further divided into a certain number of zones $z \in Z$ to better represent the system's regional/spatial characteristics. There is a specific power injection losses coefficient $L_{z,m,t}$ depending on zone $z \in Z$ and the load level of each time period. Furthermore, there is an upper bound on the allowable corridor flow, $FL_{s,s',m,t}$, between each interconnected pair of subsystems $s \in S^{s'}$. The interconnection capacity with the neighboring power system constitutes a decision variable whose bounds are determined by CL_f, where f are possible capacity blocks, and characterized by a specific unit investment cost INV_f. The studied power system is also interconnected with other power systems $n \in N$, each of which has an interconnection with a specific subsystem $n \in N^s$ (and zone $n \in N^z$) of the studied system.
- A set of power generating units $g \in G$ is installed in each subsystem $g \in G^s$ (or zone $g \in G^z$). This set includes thermal units $g \in G^{th}$, hydroelectric units $g \in G^h$, (both referred to as hydrothermal ones $g \in G^{hth}$) and renewable units $g \in G^{res}$. Each renewable unit $g \in G^{res}$ is characterized by a specific availability factor in each zone and time period, $AF_{g,z,m,t}$. Each unit $g \in G$ is characterized by a specific available power capacity $PC_{g,m,t}$. The available power capacity of each hydrothermal unit $g \in G^{hth}$ is divided into a number of blocks $b \in B$, $PCB_{g,b,m,t}$ to fully represent the operational characteristics of each unit and the real operation of power markets. In each time period and for each power capacity block, each hydrothermal power generating unit provides a specific amount of energy (to be determined by the optimization process) at a specific price (marginal cost), $CB_{g,b,m,t}$ (incorporating variable operating and maintenance cost, fuel cost, and CO_2 emissions cost) in order for the power demand in each subsystem and time period, $D_{s,m,t}$, to be covered. Apart from the priced component of each unit's energy offer function, there can be a non-priced one (zero marginal cost), $NP_{g,m,t}$, including mandatory hydroelectric injection, power injection from renewable units, and power contribution from commissioning units. The same rule applies to both electricity imports from each interconnected system, $n \in N^s$ (or zone $n \in N^z$), and load representatives such as power exports to other interconnected systems $n \in N^s$ (or zone $n \in N^z$), and pumping load $e \in E$. More specifically, the power capacities of each interconnection $n \in S^s$ and pumping load $e \in E^s$, are divided into certain blocks ($IP_{n,b,m,t}$ for imports, $EP_{n,b,m,t}$ for exports, and $PMB_{e,b,m,t}$ for pumping load), having a certain marginal cost $CIP_{n,b,m,t}$ for imports, and a given bid $CEP_{n,b,m,t}$ for exports and $CPM_{e,b,m,t}$ for pumped storage units.
- With reference to the operational cycle of each hydrothermal unit $g \in G^{hth}$: after a shut-down decision has been taken for each unit, it has to remain off (non-operational) for at least T_g^{down} hours, i.e., it is associated with a specific minimum down time. A certain cost is associated with the shut-down decision of each unit $g \in G^{hth}$, SDC_g. According to the real non-operational time of each unit $g \in G^{hth}$, T_g^{rdn}, there are three available start-up types $w \in W$ $\{W : hot, warm, cold\}$ when a start-up decision is determined by the model. Moreover, there are specific time limits after which each unit $g \in G^{hth}$ changes stand-by condition, including the non-operational time before going from hot to warm stand-by condition $\left(T_g^{htw}\right)$, and the corresponding one before going from warm to cold stand-by condition $\left(T_g^{wtc}\right)$. Furthermore, an extended time period in the past (typically higher than the maximum reservation time of all thermal units' cold start-up), T_g^{past}, is also considered in order for the model to effectively connect the prior operational status of all the units with the decisions to be determined by the optimization process. After the determination of the appropriate start-up type decision, each unit enters the synchronization phase (zero power output), having a duration of $T_g^{sync,w}$ hours, and followed by the soak phase with a duration of $T_g^{soak,w}$ hours and during which unit's power output equals P_g^{soak}. The duration of both phases is dependent on the selected start-up type decision $w \in W$. After the completion of the soak phase, each unit $g \in G^{hth}$ enters the dispatchable phase, wherein its power output can range from its technical minimum, P_g^{min}, to its technical maximum, P_g^{max}, or from $P_g^{min,sc}$ to $P_g^{max,sc}$, if that unit is selected for providing secondary reserve (see Fig. 1). During that phase, each unit is characterized by specific up, R_g^{up}, and down, R_g^{down}, ramp rates, or, R_g^{sc}, when providing secondary reserve (up and down). The last operational stage of each unit $g \in G^{hth}$ is that of desynchronization with a duration of T_g^{desyn} hours. A unit $g \in G^{hth}$ is considered operational when it operates in each one of the aforementioned phases, i.e., synchronization, soak, dispatch and desynchronization. The total operational time of each unit must be greater than or equal to its minimum up time, T_g^{up} in order to be allowed to shut-down.
- The power system's requirements include: (i) electricity demand requirements in each subsystem and time period, $D_{s,m,t}$, (ii) primary-up reserve requirements in each time period,

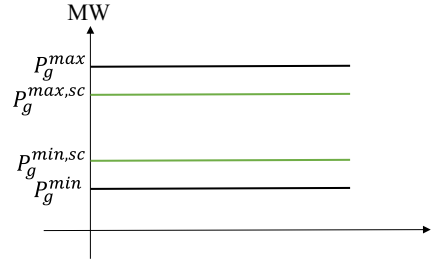

Fig. 1. Power output limits of each hydrothermal unit (MW).

$R1^{up}_{m,t}$, (iii) secondary-up, $R2^{up}_{m,t}$, and secondary-down, $R2^{down}_{m,t}$, reserve requirements in each time period, (iv) fast secondary-up, $FR2^{up}_{m,t}$, and fast secondary-down, $FR2^{down}_{m,t}$, reserve requirements in each time period, and (v) tertiary reserve requirements in each time period, $R3_{m,t}$.

- When it comes to power reserve provision capabilities, each unit $g \in G^{hth}$ is identified based on: (i) upper bound on the provision of primary reserve, $R1_g$, (ii) upper bound on the provision of secondary reserve, $R2_g$, and (iii) upper bound on the provision of tertiary spinning, $R3^{sp}_g$, and non-spinning reserve, $R3^{nsp}_g$. Each unit's energy reserve offer has a certain price, i.e., $RC1_{g,m,t}$ for the primary energy reserve, and $RC2_{g,m,t}$ for the secondary range energy offer, while tertiary energy offer is non-priced.

3. Mathematical formulation

3.1. Objective function

The proposed objective function is based on the mid-term market operation, namely the minimization of the total annual operational cost of the studied power system, based on the evolution of generation and network elements. In addition, it also incorporates the investment cost for critical energy developments, such as the interconnection cost. Therefore, the model's objective function includes: (i) marginal production cost of the power units incorporating fuel cost, variable operating and maintenance (O&M) cost, and CO_2 emission allowances cost, (ii) power imports cost, (iii) power exports revenues, (iv) pumping load revenues, (v) units' shut-down cost, (vi) reserves provision cost, and (vii) annualized interconnection investment cost for the implementation of the electricity interconnection, as represented by Eq. (1).

$$
\begin{aligned}
\textbf{Min } Cost^{annual} = {} & \overbrace{\sum_{g\in(G^{hth}\cap G^{z})}\sum_{z\in Z}\sum_{b\in B}\sum_{m\in M}\sum_{t\in T}(pb_{g,b,m,t}\cdot CB_{g,b,m,t}\cdot L_{z,m,t}\cdot Dur_m)}^{\text{Marginal production cost}} \\
& + \overbrace{\sum_{n\in N^{z}}\sum_{z\in Z}\sum_{b\in B}\sum_{m\in M}\sum_{t\in T}(imb_{n,b,m,t}\cdot CIP_{n,b,m,t}\cdot L_{z,m,t}\cdot Dur_m)}^{\text{Power imports cost}} \\
& - \overbrace{\sum_{n\in N^{z}}\sum_{z\in Z}\sum_{b\in B}\sum_{m\in M}\sum_{t\in T}(exb_{n,b,m,t}\cdot CEP_{n,b,m,t}\cdot Dur_m)}^{\text{Power exports revenues}} \\
& - \overbrace{\sum_{e\in E^{z}}\sum_{z\in Z}\sum_{b\in B}\sum_{m\in M}\sum_{t\in T}(pmb^{pum}_{e,b,m,t}\cdot CPM_{e,b,m,t}\cdot Dur_m)}^{\text{Pumping load revenues}} + \overbrace{\sum_{g\in G^{hth}}\sum_{m\in M}\sum_{t\in T}(x^{sd}_{g,m,t}\cdot SDC_g\cdot Dur_m)}^{\text{Shut-down cost}} \\
& + \overbrace{\sum_{g\in G^{hth}}\sum_{m\in M}\sum_{t\in T}[(r1^{up}_{g,m,t}\cdot RC1_{g,m,t}\cdot Dur_m)+(r2^{up}_{g,m,t}+r2^{down}_{g,m,t})\cdot RC2_{g,m,t}\cdot Dur_m]}^{\text{Reserves provision cost}} \\
& + \overbrace{\sum_{s\in(S^{IS}\cap S^{CR})}\sum_{s'\neq s\in(S^{IS}\cap S^{CR})}\sum_{f}\left(cfl_{s,s',f}\cdot\frac{INV_f}{2}\right)}^{\text{Annualized interconnection investment cost}}
\end{aligned}
\tag{1}
$$

3.2. Model constraints

Constraints (2)–(12) represent the typical operational cycle of a hydrothermal unit $g \in G^{hth}$ incorporated in the formulation of the unit commitment problem (UCP). The operating phases include those of start-up decision, synchronization, soak, and desynchronization. Minimum up and down times are also modeled, while the power output limits of each hydrothermal unit is represented in Fig. 1. More specifically:

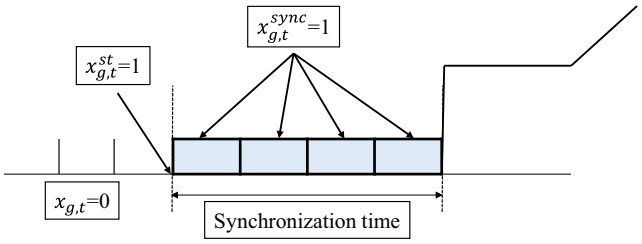

Fig. 2. Modeling of the synchronization phase.

3.2.1. Start-up decision constraints

$$x^{st,w}_{g,m,t} \leqslant \sum_{t'=t-T^{max}_{g}+1}^{t-T^{min}_{g}} x^{sd}_{g,m,t'} \quad \forall w\in W,\ g\in G^{hth},\ m\in M,\ t\in T \tag{2}$$

$$x^{st}_{g,m,t} = \sum_{w\in W} x^{st,w}_{g,m,t} \quad \forall g\in G^{hth},\ m\in M,\ t\in T \tag{3}$$

After a shut-down decision has been taken $\left(x^{st}_{g,m,t}=1\right)$, and the unit $g \in G^{hth}$ remains non-operational $(x_{g,m,t}=0)$ for T^{rdn}_g hours, an appropriate start-type decision can be taken for each unit in each time period according to the amount of that time, T^{rdn}_g, as described by constraints (2) [23]. Eq. (3) guarantees that a unit $g \in G^{hth}$ can start-up with only one start-up type $w \in W$ at each time period.

3.2.2. Synchronization operational stage constraints

$$x^{sync,w}_{g,m,t} \leqslant \sum_{t'=t-T^{sync,w}_{g}+1}^{t} x^{st,w}_{g,m,t'} \quad \forall w\in W,\ g\in G^{hth},\ m\in M,\ t\in T \tag{4}$$

$$x^{sync}_{g,m,t} = \sum_{w\in W} x^{sync,w}_{g,m,t} \quad \forall g\in G^{hth},\ m\in M,\ t\in T \tag{5}$$

Once the proper start-up type decision is taken ($x^{st,w}_{g,m,t} = x^{st}_{g,m,t} = 1$ for a certain $w \in W$), each unit $g \in G^{hth}$ enters the synchronization phase ($x^{sync,w}_{g,m,t} = x^{sync}_{g,m,t} = 1$ for a certain $w \in W$) with a duration of $T^{sync,w}_g$ hours, as described by constraints (4) and (5). Note that the power output of each unit $g \in G^{hth}$ during the synchronization phase equals zero, as can be observed in Fig. 2.

3.2.3. Soak operational stage constraints

$$x^{soak,w}_{g,m,t} \leqslant \sum_{t'=t-T^{sync,w}_{g}-T^{soak,w}_{g}+1}^{t-T^{sync,w}_{g}} x^{st,w}_{g,m,t'} \quad \forall w \in W,\ g \in G^{hth},\ m \in M,\ t \in T \tag{6}$$

$$x^{soak}_{g,m,t} = \sum_{w \in W} x^{soak,w}_{g,m,t} \quad \forall g \in G^{hth},\ m \in M,\ t \in T \tag{7}$$

$$p^{soak}_{g,m,t} = P^{soak}_{g} \cdot x^{soak}_{g,m,t} \quad \forall g \in G^{hth},\ m \in M,\ t \in T \tag{8}$$

After the completion of the synchronization stage, each unit $g \in G^{hth}$ enters the soak phase ($x^{soak,w}_{g,m,t} = x^{soak}_{g,t} = 1$ for a specific $w \in W$), having a duration of $T^{soak,w}_{g}$ hours, and during which the unit's power output amounts to a fixed value, P^{soak}_{g}, as guaranteed by constraints (6)–(8) (see also Fig. 3).

3.2.4. Desynchronization operational stage constraints

$$x^{desyn}_{g,m,t} = \sum_{t'=t+1}^{t+T^{desyn}_{g}-1} x^{sd}_{g,m,t'} \quad \forall g \in G^{hth},\ m \in M,\ t \in T \tag{9}$$

$$p^{desyn}_{g,m,t} = \sum_{t'=t}^{t+T^{desyn}_{g}-1} x^{desyn}_{g,m,t} \cdot (t'-t) \cdot \frac{P^{min}_{g}}{T^{desyn}_{g}} \quad \forall g \in G^{hth},\ m \in M,\ t \in T \tag{10}$$

The next operational stage of each unit $g \in G^{hth}$ is that of dispatchable stage $\left(x^{disp}_{g,m,t} = 1\right)$, having a duration of T^{disp}_{g} hours, and during which the unit's power output can range from its technical minimum, P^{min}_{g}, to its maximum, P^{max}_{g}, subject to its technical up and down ramp rates, R^{up}_{g} and R^{down}_{g} respectively when committed, or to R^{sc}_{g} when selected for providing secondary reserve. Finally, the last possible operational stage of a unit $g \in G^{hth}$ is that of desynchronization, with a duration of T^{desyn}_{g} hours, as described by constraints (9). Eq. (10) secure that each unit's power output decreases with a particular power sequence during that phase $\left(x^{desyn}_{g,m,t} = 1\right)$, as depicted in Fig. 4.

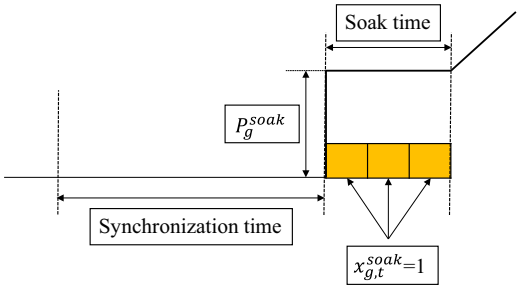

Fig. 3. Modeling of the soak phase.

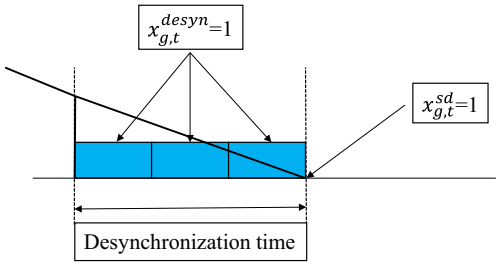

Fig. 4. Modeling of the desynchronization phase.

3.2.5. Minimum up and down time constraints

Constraints (11) and (12) model the minimum up and down times of each unit $g \in G^{hth}$ respectively, i.e., each unit $g \in G^{hth}$ must remain operational (or non-operational) in each time period $t \in T$ if it has started-up (or shut-down) during the previous $\left(T^{up}_{g}-1\right)$ (or $T^{down}_{g}-1$) hours correspondingly. In other words, the sum of $T^{sync,w}_{g}+T^{soak,w}_{g}+T^{disp}_{g}+T^{desyn}_{g}$ must be greater than or equal to the minimum up time of each unit $g \in G^{hth}$, T^{up}_{g}, and the unit's non-operational time (after being shut-down), T^{rdn}_{g}, must be greater than or equal to the minimum down time of each unit $g \in G^{hth}$, T^{down}_{g}, in order to be able to start-up again.

$$\sum_{t'=t-T^{up}_{g}+1}^{t} x^{st}_{g,m,t'} \leqslant x_{g,m,t} \quad \forall g \in G^{hth},\ m \in M,\ t \in T \tag{11}$$

$$\sum_{t'=t-T^{down}_{g}+1}^{t} x^{sd}_{g,m,t'} \leqslant 1 - x_{g,m,t} \quad \forall g \in G^{hth},\ m \in M,\ t \in T \tag{12}$$

3.2.6. Logical constraints of unit commitment

Constraints (13) guarantee that each unit $g \in G^{hth}$ can only be at one of the possible operational phases in each time period $t \in T$ when committed. Constraints (14) and (15) describe the start-up $\left(x^{st}_{g,m,t}\right)$ and shut-down $\left(x^{sd}_{g,m,t}\right)$ decision of each unit $g \in G^{hth}$ during each time period. As constraints (15) state, a start-up and a shut-down decision cannot be taken simultaneously in each time period for a unit $g \in G^{hth}$. Constraints (16) ensure that each unit $g \in G^{hth}$ is able to contribute to secondary reserve if and only if operates in the dispatchable phase.

$$x_{g,m,t} = x^{sync}_{g,m,t} + x^{soak}_{g,m,t} + x^{disp}_{g,m,t} + x^{desyn}_{g,m,t} \quad \forall g \in G^{hth},\ m \in M,\ t \in T \tag{13}$$

$$x^{st}_{g,m,t} - x^{sd}_{g,m,t} = x_{g,m,t} - x_{g,m,t-1} \quad \forall g \in G^{hth},\ m \in M,\ t \in T \tag{14}$$

$$x^{st}_{g,m,t} + x^{sd}_{g,m,t} \leqslant 1 \quad \forall g \in G^{hth},\ m \in M,\ t \in T \tag{15}$$

$$x^{sec}_{g,m,t} \leqslant x^{disp}_{g,m,t} \quad \forall g \in G^{hth},\ m \in M,\ t \in T \tag{16}$$

3.2.7. Energy offer constraints

Eq. (17) describe the power output of each unit $g \in G^{hth}$ being divided into two parts: (i) fixed (non-priced) component including mandatory hydro power injection and/or hydrothermal power injection from units operating under commissioning status in each time period ($NP_{g,m,t}$), and (ii) priced component based on the energy offer per power capacity block (energy offer function) of each unit $g \in G^{hth}$ in each time period ($pb_{g,b,m,t}$). Power injection provided by renewable energy technologies is also non-priced, based on the availability factor of each renewable energy resource (e.g., wind, solar) in each zone and time period and provided by constraints (18). Constraints (19) define that the portion of each block $b \in B$ of each existing hydrothermal unit's energy offer function being dispatched in each time period, $pb_{g,b,m,t}$, must not exceed the size of the corresponding step of unit's energy offer function.

$$p_{g,m,t} = NP_{g,m,t} + \sum_{b \in B} pb_{g,b,m,t} \quad \forall g \in G^{hth},\ m \in M,\ t \in T \tag{17}$$

$$p_{g,m,t} = AF_{g,z,m,t} \cdot PC_{g,m,t} \quad \forall g \in G^{res},\ z \in Z,\ m \in M,\ t \in T \tag{18}$$

$$pb_{g,b,m,t} \leqslant PCB_{g,b,m,t} \quad \forall g \in G^{hth},\ b \in B,\ m \in M,\ t \in T \tag{19}$$

3.2.8. Power imports, exports and pumped storage constraints

Constraints (20) and (21) describe the power injection (withdrawal) of imports (exports) from (to) interconnected power system

$n \in N$ during each time period respectively. Eq. (22) define the power withdrawal of pumped storage units $e \in E$ in each time period. Constraints (23) and (24) define that the portion of each block $b \in B$ of each interconnected system's imports (exports) energy offer (bid) function in each time period, $imb_{n,b,m,t}$ ($exb_{n,b,m,t}$), must not exceed the size of the corresponding step of each interconnected system's imports (exports) energy offer function, $IP_{n,b,m,t}$ ($EP_{n,b,m,t}$). Finally, constraints (25) express the same for pumped storage units $e \in E$ as constraints (24) for power exports.

$$im_{n,m,t} = \sum_{b \in B} imb_{n,b,m,t} \quad \forall n \in N,\ m \in M,\ t \in T \tag{20}$$

$$ex_{n,m,t} = \sum_{b \in B} exb_{n,b,m,t} \quad \forall n \in N,\ m \in M,\ t \in T \tag{21}$$

$$pm^{pum}_{e,m,t} = \sum_{b \in B} pmb^{pum}_{e,b,m,t} \quad \forall e \in E,\ m \in M,\ t \in T \tag{22}$$

$$imb_{n,b,m,t} \leqslant IP_{n,b,m,t} \quad \forall n \in N,\ b \in B,\ m \in M,\ t \in T \tag{23}$$

$$exb_{n,b,m,t} \leqslant EP_{n,b,m,t} \quad \forall n \in N,\ b \in B,\ m \in M,\ t \in T \tag{24}$$

$$pmb^{pum}_{e,b,m,t} \leqslant PMB_{e,b,m,t} \quad \forall e \in E,\ b \in B,\ m \in M,\ t \in T \tag{25}$$

3.2.9. Net power injections and power output constraints

Eqs. (26) and (27) describe the net power injections from both units $g \in G^Z$ and the interconnected power systems $n \in N^z$ (imports) by considering the injection losses coefficient of each zone $z \in Z$ in each time period $t \in T$. Constraints (28)–(30) define the power output limits of each unit $g \in G^{hth}$ in each operational phase.

$$p^{net}_{g,m,t} = L_{z,m,t} \cdot p_{g,m,t} \quad \forall g \in G^Z,\ z \in Z,\ m \in M,\ t \in T \tag{26}$$

$$im^{net}_{n,m,t} = L_{z,m,t} \cdot im_{n,m,t} \quad \forall n \in N^z,\ z \in Z,\ m \in M,\ t \in T \tag{27}$$

$$p_{g,m,t} - r2^{down}_{g,m,t} \geqslant 0 \cdot x^{sync}_{g,m,t} + p^{soak}_{g,m,t} + p^{desyn}_{g,m,t} + P^{min}_{g} \cdot \left(x^{disp}_{g,m,t} - x^{sec}_{g,m,t}\right) + P^{min,sc}_{g} \cdot x^{sec}_{g,m,t} \quad \forall g \in G^{hth},\ m \in M,\ t \in T \tag{28}$$

$$p_{g,m,t} + r2^{up}_{g,m,t} \geqslant 0 \cdot x^{sync}_{g,m,t} + p^{soak}_{g,m,t} + p^{desyn}_{g,m,t} + P^{max}_{g} \cdot \left(x^{disp}_{g,m,t} - x^{sec}_{g,m,t}\right) + P^{max,sc}_{g} \cdot x^{sec}_{g,m,t} \quad \forall g \in G^{hth},\ m \in M,\ t \in T \tag{29}$$

$$p_{g,m,t} + r1^{up}_{g,m,t} + r2^{up}_{g,m,t} + r3^{sp}_{g,m,t} \geqslant 0 \cdot x^{sync}_{g,m,t} + p^{soak}_{g,m,t} + p^{desyn}_{g,m,t} + P^{max}_{g} \cdot x^{disp}_{g,m,t} \quad \forall g \in G^{hth},\ m \in M,\ t \in T \tag{30}$$

3.2.10. Reserve-type constraints

Constraints (31) define the upper bounds of primary-up reserve of each unit $g \in G^{hth}$, subject to the decision of its operation (or not) in the dispatchable operational stage $\left(x^{disp}_{g,m,t}\right)$. Constraints (32) ensure that the sum of the provisions of each unit $g \in G^{hth}$ in secondary-up and down reserves must be less than or equal to the maximum allowable secondary reserve contribution of each unit $g \in G^{hth}$, $R2_g$, subject to the decision of its contribution (or not) to the secondary reserve $\left(x^{sec}_{g,m,t}\right)$. Constraints (33) and (34) define the upper bounds of tertiary spinning and non-spinning reserves of each unit $g \in G^{hth}$ correspondingly, subject to the decision of its operation (or not) in the dispatchable phase $\left(x^{disp}_{g,m,t}\right)$, and to the decision for the provision (or not) of tertiary non-spinning reserve in each time period $\left(x^{3ns}_{g,m,t}\right)$ respectively. Constraints (35) ensure that the provision of each unit $g \in G^{hth}$ in the tertiary non-spinning reserve must be greater than or equal to the unit's technical minimum $\left(P^{min}_{g}\right)$. Constraints (36) define that each unit $g \in G^{hth}$ is able to provide tertiary non-spinning reserve if and only if is non-operational. Eq. (37) state that the total provision of each unit $g \in G^{hth}$ in tertiary reserve amounts to the sum of its contribution to tertiary spinning and non-spinning reserves. Constraints (38) guarantee that the contribution of each unit $g \in G^{hth}$ to the fast secondary-up reserve within a period of 1 min, must be less than or equal to its contribution to the secondary-up reserve. Furthermore, constraints (39) define an upper limit on the fast secondary-up reserve. Constraints (40) and (41) define the same bounds for the fast secondary-down reserve of each unit $g \in G^{hth}$ as constraints (38) and (39) for the fast secondary-up reserve correspondingly.

$$r1^{up}_{g,m,t} \leqslant R1_g \cdot x^{disp}_{g,m,t} \quad \forall g \in G^{hth},\ m \in M,\ t \in T \tag{31}$$

$$r2^{up}_{g,m,t} + r2^{down}_{g,m,t} \leqslant R2_g \cdot x^{sec}_{g,m,t} \quad \forall g \in G^{hth},\ m \in M,\ t \in T \tag{32}$$

$$r3^{sp}_{g,m,t} \leqslant R3^{sp}_{g} \cdot x^{disp}_{g,m,t} \quad \forall g \in G^{hth},\ m \in M,\ t \in T \tag{33}$$

$$r3^{nsp}_{g,m,t} \leqslant R3^{nsp}_{g} \cdot x^{3ns}_{g,m,t} \quad \forall g \in G^{hth},\ m \in M,\ t \in T \tag{34}$$

$$r3^{nsp}_{g,m,t} \geqslant P^{min}_{g} \cdot x^{3ns}_{g,m,t} \quad \forall g \in G^{hth},\ m \in M,\ t \in T \tag{35}$$

$$x^{3ns}_{g,m,t} \leqslant 1 - x_{g,m,t} \quad \forall g \in G^{hth},\ m \in M,\ t \in T \tag{36}$$

$$r3_{g,m,t} = r3^{sp}_{g,m,t} + r3^{nsp}_{g,m,t} \quad \forall g \in G^{hth},\ m \in M,\ t \in T \tag{37}$$

$$fr2^{up}_{g,m,t} \leqslant r2^{up}_{g,m,t} \quad \forall g \in G^{hth},\ m \in M,\ t \in T \tag{38}$$

$$fr2^{up}_{g,m,t} \leqslant R^{sc}_{g} \cdot 1min \quad \forall g \in G^{hth},\ m \in M,\ t \in T \tag{39}$$

$$fr2^{down}_{g,m,t} \leqslant r2^{down}_{g,m,t} \quad \forall g \in G^{hth},\ m \in M,\ t \in T \tag{40}$$

$$fr2^{down}_{g,m,t} \leqslant R^{sc}_{g} \cdot 1min \quad \forall g \in G^{hth},\ m \in M,\ t \in T \tag{41}$$

3.2.11. System's energy requirements

Constraints (42)–(47) model the system's requirements for all energy reserve types, i.e., primary-up, secondary-up and down, tertiary, as well as fast secondary-up and down respectively in each time period $t \in T$. These requirements (primary-up reserve requirements are considered to remain constant) are assumed to increase linearly with the total installed capacity of renewable units.

$$\sum_{g \in G^{hth}} r1^{up}_{g,m,t} \geqslant R1^{up}_{m,t} \quad \forall m \in M,\ t \in T \tag{42}$$

$$\sum_{g \in G^{hth}} r2^{up}_{g,m,t} \geqslant R2^{up}_{m,t} + \alpha \cdot \left(IC^{tot}_{res} - IC^{int}_{res}\right) \cdot \frac{R2^{up}_{m,t}}{R2^{up}_{m,t} + R2^{down}_{m,t}} \quad \forall m \in M,\ t \in T \tag{43}$$

$$\sum_{g \in G^{hth}} r2^{down}_{g,m,t} \geqslant R2^{down}_{m,t} + \beta \cdot \left(IC^{tot}_{res} - IC^{int}_{res}\right) \cdot \frac{R2^{down}_{m,t}}{R2^{up}_{m,t} + R2^{down}_{m,t}} \quad \forall m \in M,\ t \in T \tag{44}$$

$$\sum_{g\in G^{hth}} r3_{g,m,t} \geqslant R3_{m,t} + \gamma \cdot \left(IC^{tot}_{res} - IC^{int}_{res}\right) \quad \forall m \in M,\ t \in T \tag{45}$$

$$\sum_{g\in G^{hth}} fr2^{up}_{g,m,t} \geqslant FR2^{up}_{m,t} + \delta \cdot \left(IC^{tot}_{res} - IC^{int}_{res}\right) \cdot \frac{FR2^{up}_{m,t}}{FR2^{up}_{m,t} + FR2^{down}_{m,t}}$$
$$\forall m \in M,\ t \in T \tag{46}$$

$$\sum_{g\in G^{hth}} fr2^{down}_{g,m,t} \geqslant FR2^{down}_{m,t} + \varepsilon \cdot \left(IC^{tot}_{res} - IC^{int}_{res}\right) \cdot \frac{FR2^{down}_{m,t}}{FR2^{up}_{m,t} + FR2^{down}_{m,t}}$$
$$\forall m \in M,\ t \in T \tag{47}$$

3.2.12. Ramp rate constraints

According to constraints (48) and (49), each unit $g \in G^{hth}$ is able to increase or decrease its power output according to specific ramp rates (up and down) in each time period, the values of which are contingent on the unit's operational status, i.e., if it provides secondary reserve or not $\left(x^{sec}_{g,m,t}\right)$.

$$p_{g,m,t} - p_{g,m,t-1} \leqslant \left(1 - x^{sec}_{g,m,t}\right) \cdot R^{up}_{g} + R^{sc}_{g} \cdot x^{sec}_{g,m,t} \cdot 60$$
$$\forall g \in G^{hth},\ m \in M,\ t \in T \tag{48}$$

$$p_{g,m,t-1} - p_{g,m,t} \leqslant \left(1 - x^{sec}_{g,m,t}\right) \cdot R^{down}_{g} + R^{sc}_{g} \cdot x^{sec}_{g,m,t} \cdot 60$$
$$\forall g \in G^{hth},\ m \in M,\ t \in T \tag{49}$$

3.2.13. Corridor limits

Constraints (50) define that the corridor flow between two interconnected subsystems $s, s' \in S^{s}$, must be less than or equal to the maximum available power capacity of the corridor $(FL_{s,s',m,t})$ in each time period. Constraints (51)–(54) define the capacity bounds for a proposed electricity interconnection subject to the decision for its construction or not.

$$f_{s,s',m,t} \leqslant FL_{s,s',m,t} \quad \forall (s,s') \in S^{IS},\ m \in M,\ t \in T \tag{50}$$

$$f_{s,s',m,t} \leqslant \sum_{f\in F} cfl_{s,s',f} \quad \forall (s,s') \in (S^{IS} \cap S^{CR}),\ m \in M,\ t \in T \tag{51}$$

$$cfl_{s,s',f} \leqslant CL_{f} \cdot y_{f} \quad \forall (s,s') \in \left(S^{IS} \cap S^{CR}\right),\ f \in F \tag{52}$$

$$cfl_{s,s',f} \geqslant CL_{f-1} \cdot y_{f} \quad \forall (s,s') \in \left(S^{IS} \cap S^{CR}\right),\ f \in F \tag{53}$$

$$\sum_{f\in F} y_{f} \leqslant 1 \tag{54}$$

3.2.14. Energy demand balance

Eq. (55) describe the energy demand balance of the overall power system. More specifically, net power injection from all power units $\left(\sum_{g\in G^{s}} p^{net}_{g,m,t}\right)$ plus net electricity flow rates $\left(\sum_{s'\in S^{s}} f_{s',s,m,t} - \sum_{s'\in S^{s}} f_{s,s',m,t}\right)$ and net electricity imports $\left(\sum_{n\in N^{s}} im^{net}_{n,m,t} - \sum_{n\in N^{s}} ex_{n,m,t}\right)$ to each subsystem $s \in S$, must be equal to the electricity demand of each sector $D_{s,m,t}$ and the pumping load, $\sum_{e\in E} pm^{pum}_{e,m,t}$.

$$\sum_{g\in G^{s}} p^{net}_{g,m,t} + \overbrace{\sum_{n\in N^{s}} im^{net}_{n,m,t} - \sum_{n\in N^{s}} ex_{n,m,t}}^{net\ electricity\ imports}$$
$$+ \overbrace{\sum_{s'\in S^{s}} f_{s',s,m,t} - \sum_{s'\in S^{s}} f_{s,s',m,t}}^{net\ electricity\ flow\ rates}$$
$$= D_{s,m,t} + \sum_{e\in E^{s}} pm^{pum}_{e,m,t} \quad \forall s \in S,\ m \in M,\ t \in T \tag{55}$$

The overall problem is formulated as an MILP (mixed-integer linear programming) problem, involving the cost minimization objective function (1) subject to constraints (2)–(55).

4. Case study

The inter-zonal Greek power system including the interconnected system (mainland), i.e., the North and the South subsystem, and that of Crete, is taken into account. Note also that the North subsystem is divided into two zones (Zones 1–2) and the South subsystem is split into 3 zones (Zones 3–5) to reflect the regional characteristics of the national system in a more analytical way. Fig. 5 portrays a graphical representation of the inter-zonal Greek power system.

As far as the mix of the installed capacity is concerned, the projected capacity of 2020 is considered, on the grounds that it is the year that the electricity interconnection between Crete and mainland is going to be implemented given that the decision for its construction is taken in 2016 (see Fig. 5).

With regard to the interconnected power system, fifty hydrothermal power units are taken into consideration, including eleven lignite-fired units with a power capacity of 3.4 GW, four oil-fired power plants with a total capacity of 698 MW, seventeen natural-gas fired (both natural gas combined cycle and natural gas open cycle units) power plants with a cumulative capacity of 5.7 GW, and eighteen hydroelectric units whose capacity equals 3.1 GW (see Table 1).

With regard to the installed capacity of renewables in the interconnected power system, this include 3 GW of wind turbines, 3 GW of photovoltaics, 127.7 MW of high-efficiency combined heat and power units, 200 MW of biomass units, and 300 MW of small hydroelectric units in total (see Fig. 6).

The main operational and economic characteristics of the installed units are available in our previous contributions [23–25]. These data include: (i) representative ramp rates, maximum contribution in primary, secondary, spinning and non-spinning tertiary reserve per technology type, (ii) representative power outputs in different operational stages (automatic generation control, soak phase, dispatch phase) per technology type, (iii) representative CO_2 emission factor per capacity block and technology type, (iv) representative non-operational time intervals before each representative unit's transition to the next standby condition and shut-down cost, and (v) representative synchronization (per start-up type), soak (per start-up type), desynchronization, minimum up and down time per technology type.

When it comes to the power system of Crete, oil-fired units comprise the dominant power technology with a total capacity of around 700 MW. With regard to RES penetration in Crete, there is a relatively small installed capacity amounting to 272.6 MW in total, of which 194.3 MW account for wind turbines and 78.3 MW for photovoltaics [26–28]. However, since there exists high uncertainty regarding the evolution of the renewables' installed capacities in the island of Crete and in order to mainly examine their impacts on the implementation of the electricity interconnection of the island with the mainland (South subsystem), as well as on other operational details, seven scenarios with different capacities of the renewable technologies in the island have been studied, as presented in Table 2.

The interconnection of the Crete Island is the most important energy infrastructure development that the Independent Power Transmission System Operator S.A. (ADMIE) has undertaken to implement in its Ten Year Network Development Plan (TYNDP). The Regulatory Authority of Energy (RAE) has approved through its 560/2013 decision the TYNDP for the period 2014–2023, mentioning – that ADMIE has to make a final decision – until the sub-

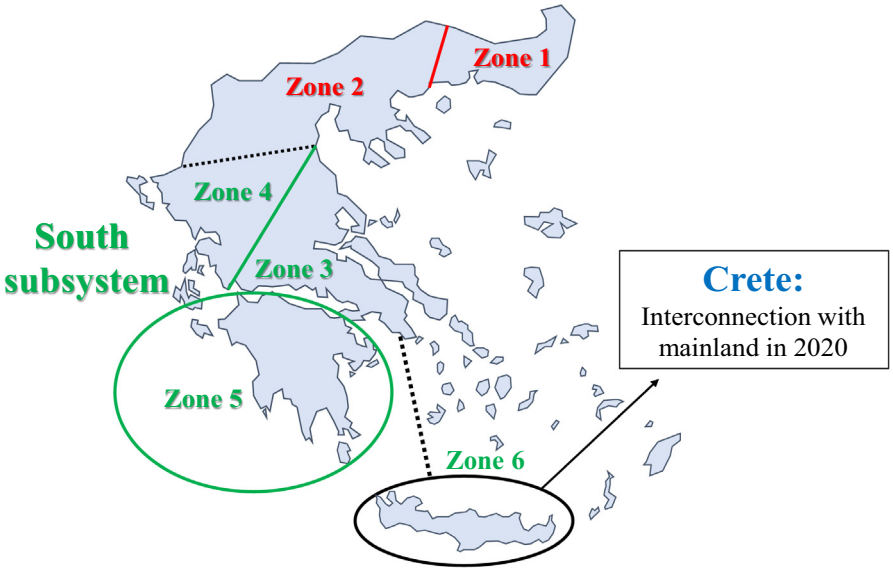

Fig. 5. Graphical representation of the inter-zonal Greek power system.

Table 1
Hydrothermal installed capacity per technology type and zone in the Greek interconnected power system (MW) in 2015.

Technology type	Zone 1	Zone 2	Zone 3	Zone 4	Zone 5
Lignite	0	2906	0	0	511
Natural gas	476	390	4048.1	0	811
Oil	0	0	698	0	0
Hydro	0	1495	120	1433.6	64

Table 2
Installed capacity of renewables (wind and photovoltaics) in Crete (Zone 6) per scenario (MW).

Scenario	Wind in Zone 6	Photovoltaics in Zone 6
Scenario 0	0	0
Scenario 1	194.4	78.3
Scenario 2	400	100
Scenario 3	800	200
Scenario 4	1200	300
Scenario 5	1600	400
Scenario 6	2000	500

mission of the TYNDP for 2015–2024 – on the following critical issues concerning the Crete interconnection: identification of the interconnection nodes in the mainland and the Crete electric system, and identification of the dimension of the interconnection cable (e.g. 2 cables of 500 MW each).

Fig. 7 presents the main interconnection options that ADMIE has identified in its recent TYNDP. This concerns the DC interconnection with a capacity of 1GW, either to Attica region (Zone 3) or to Peloponnese (Zone 4). Although the interconnection with Peloponnese is a shorter and cheaper option, it is not the preferable, as the environmental licensing procedure and the construction is expected to last significantly longer, as it requires major developments in the transmission system also in the mainland and not only undersea. Therefore, this option has not been examined in the upcoming scenarios, as its implementation is not related to the techno-economic outputs of the model. The economic data of the electricity interconnection, i.e., the unit investment cost per interconnection capacity block are provided in Table 3.

When it comes to neighboring grids, five countries (Albania, Bulgaria, FYROM, Turkey, and Italy) share electricity interconnec-

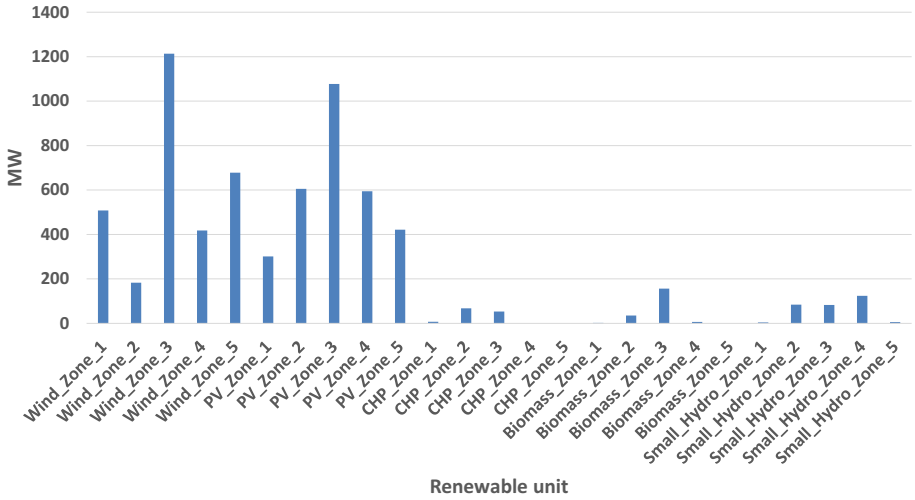

Fig. 6. Renewables' installed capacity per technology type and zone in the Greek interconnected power system (MW).

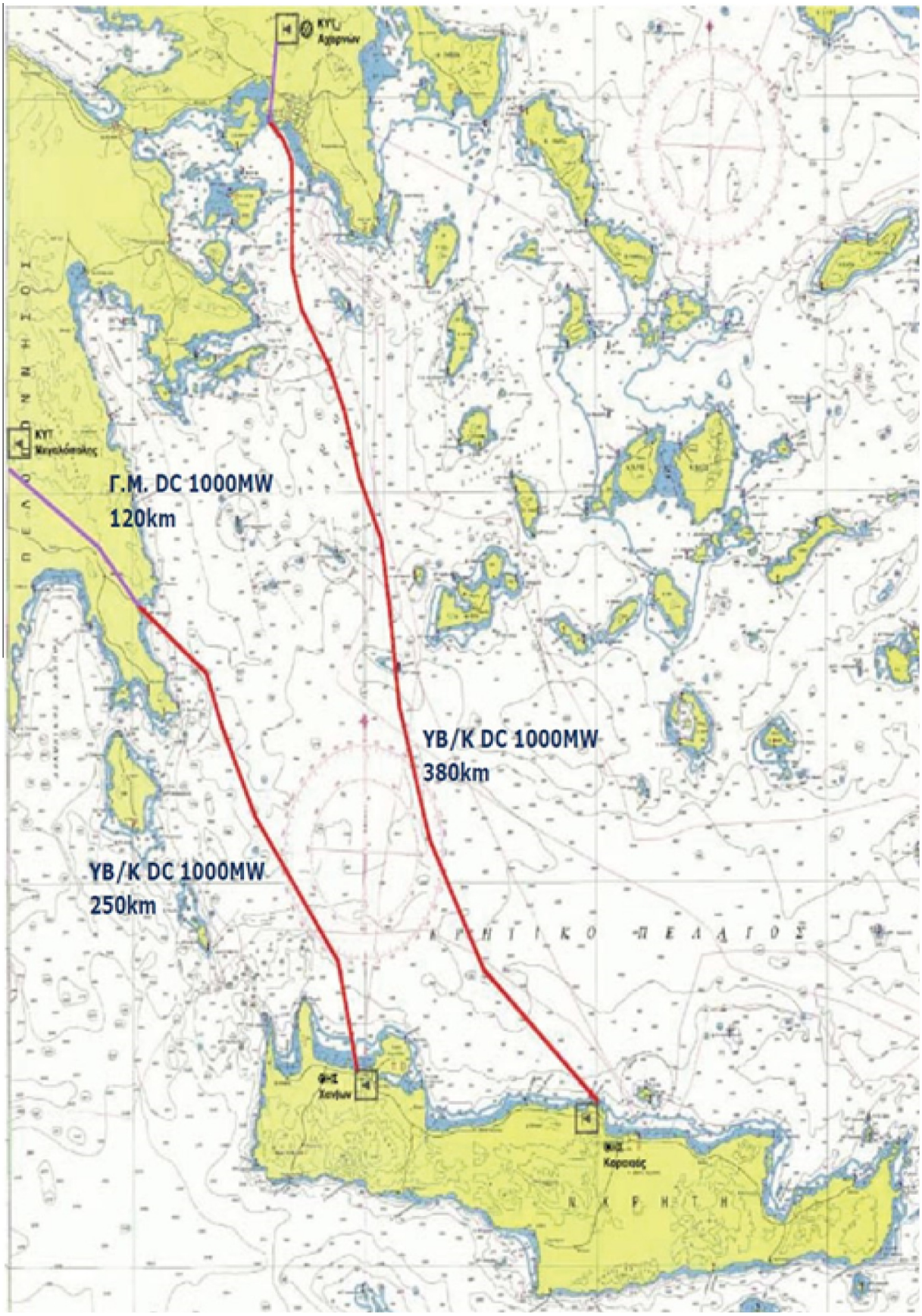

Fig. 7. Possible interconnection options of Crete with mainland [26].

Table 3
Economic data of the electricity interconnection between Crete and the South subsystem.

Interconnection capacity-IC (MW)	Unit investment cost (€/MW)
$0 \leqslant IC < 250$	141,191
$250 \leqslant IC < 500$	128,356
$500 \leqslant IC < 750$	116,687
$750 \leqslant IC < 1000$	106,079
$1000 \leqslant IC < 1250$	100,775
$1250 \leqslant IC < 1500$	95,737
$1500 \leqslant IC < 1750$	90,950
$1750 \leqslant IC < 2000$	86,402
$2000 \leqslant IC < 2250$	82,082
$2250 \leqslant IC < 2500$	77,978
$2500 \leqslant IC < 2750$	74,079
$2750 \leqslant IC < 3000$	70,375

tions with the Greek interconnected power system, of which Albania, Bulgaria and FYROM are interconnected with Zone 2 (North subsystem), Turkey with Zone 1 (North subsystem), and Italy with Zone 4 (South subsystem). The maximum allowable corridor flow between the North and the South subsystem equals 3100 MW, while the corresponding one between Crete and the South subsystem (if implemented) constitutes a decision variable determined by the mathematical model.

The examined period is one year and includes 12 representative days, one per month and at an hourly level to chiefly highlight the meteorological characteristics of the intermittent and variable energy resources. Each representative day has the duration of its corresponding month in days.

Typical values of the wind and solar availability can be found in [23], while Fig. 8 depicts the assumed availability of small hydro units in a specific zone during all the representative days (at an hourly level) of the studied year.

With regard to the power electricity demand, this amounts to 55.8 TW h at an annual level, including the interconnected system and Crete. Fig. 9 depicts a representative 24-h electricity demand profile of a typical day of January for each subsystem.

With regard to electricity trading, it is typically organized in power mandatory pools (Greece's case) or exchanges. Commonly, the preferred marketplace for short-term (daily) transactions is a day-ahead market, often referred to as forward market in the USA and as spot market in Europe [29]. This market is organized as a two-sided power auction where electricity producers, retailers, and large consumers submit offers and bids for power supply to and withdrawal from the grid, correspondingly, throughout the following day. Market participants (e.g., power plants' owners, importers, exporters) must usually submit 24 selling offers/purchasing bids in total, i.e., one for each hour of the following day. Their hourly offers/bids are typically divided into a number of blocks, each of which is associated with a specific pair of power quantity and its corresponding price. Each offer/bid is specified as a set of price–quantity pairs, indicating the amount of energy the participant is willing to sell/purchase at a given price. In order to clear the market, the market operator collects all the offers/bids

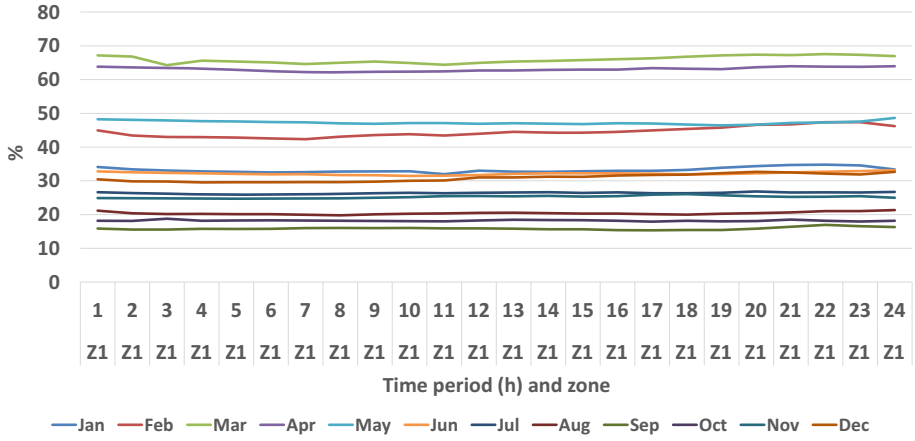

Fig. 8. Hourly availability factor (%) of small hydro units in each representative day of each month in Zone 1.

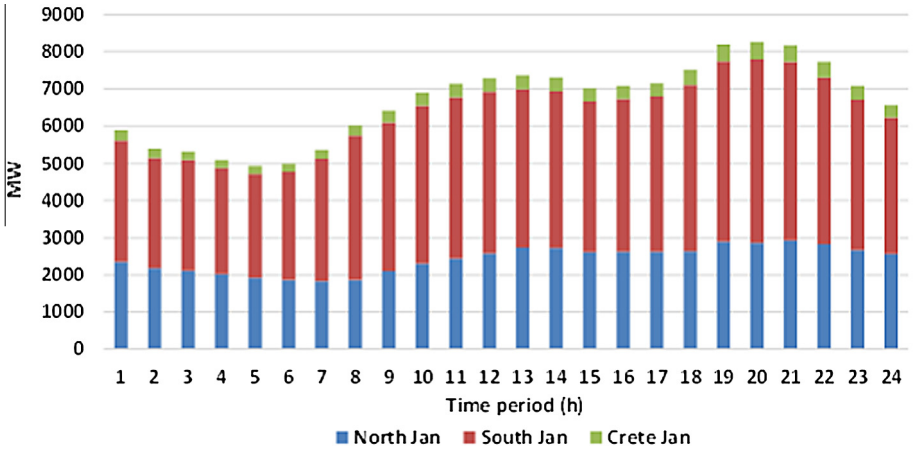

Fig. 9. Hourly power demand profile of a typical day of January for each subsystem (MW).

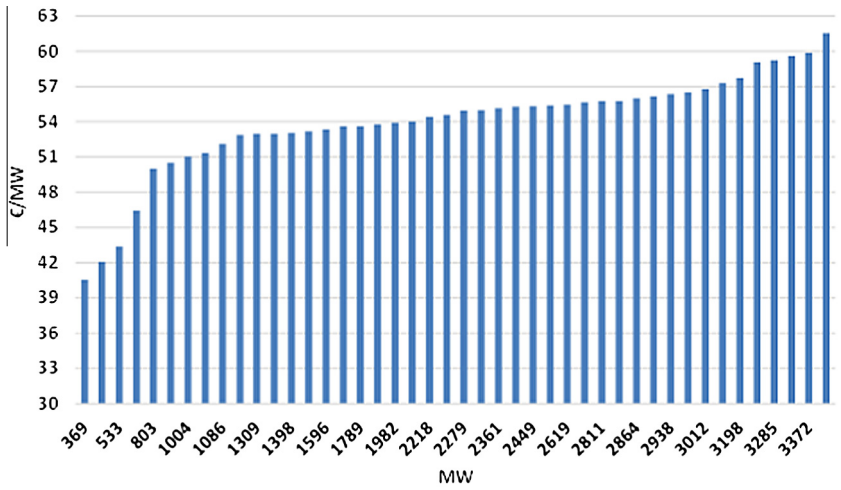

Fig. 10. Price-quantity pairs of all the available lignite-fired units.

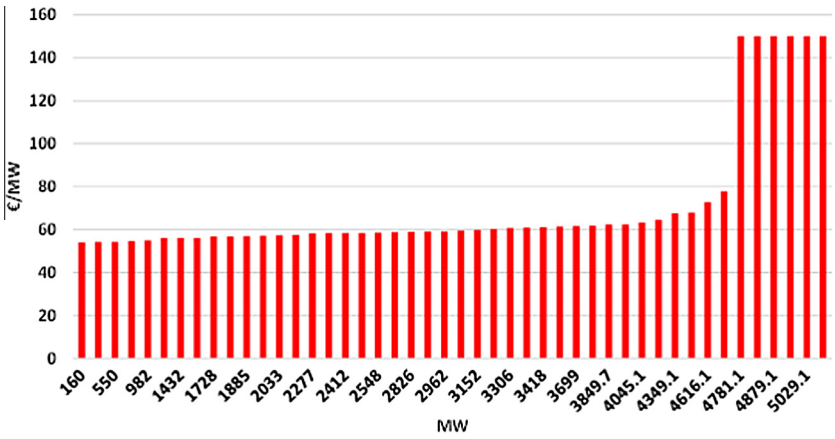

Fig. 11. Price-quantity pairs of all the available natural gas-fired units.

and determines aggregate sale and purchase curves by sorting the sale offers according to increasing prices, and the purchase bids in the inverse order. The objective of the electricity market operator refers to electricity demand and power reserves satisfaction in the most economical way. Figs. 10 and 11 depict the price-quantity pairs of all the available lignite-fired and natural gas-fired units correspondingly. These values are assumed to be identical during each representative day of each month.

Regarding the availability factor of the lignite-fired units, due to a certain maintenance period for each unit during the year, Fig. 12 portrays the total availability (%) per representative day of each month (at an hourly level) for the whole fleet of the installed lignite-fired units according to historical data and the projected maintenance period of each unit.

When it comes to the evolution of each reserve type per selected scenario, their values are different among the employed scenarios, since they are highly dependent on the degree of variability injected into the system by the renewables mix. Note that coefficients α, β, γ, δ, and ε of Eqs. (43)–(47) in Section 3 correspondingly equal 0.1 (10%).

5. Results and discussion

This section provides the results and a detailed discussion of various scenarios that have been considered. The problem has been solved to global optimality making use of the ILOG CPLEX 12.6.0.0 solver incorporated in the General Algebraic Modeling System (GAMS) tool [30]. An integrality gap of 1% has been achieved in all cases (Scenarios 0–6).

5.1. Production mix

The results indicate significant variations in terms of the electricity generation from each power technology according to each scenario, as can be seen in Fig. 13.

Lignite-fired power production constitutes the most stable power contributor, since from 18.6 TW h in Scenario 0 (at an annual level), it decreases to 18.3 TW h in Scenario 3 and 18.1 TW h in Scenario 6, a reduction of almost 3% between Scenario 0 and Scenario 6. This can be mainly attributed to the fact that it comprises the most economical fossil-fuel power generation technology.

Natural gas-fired electro-production is characterized by a sharp fall, since it decreases from 10.7 TW h in Scenario 0 to 5.4 TW h in Scenario 6, i.e., a decrease of almost 50%. It seems that natural gas units, having higher variable cost than lignite units, are the main losers, in terms of power contribution, due to the gradual and massive penetration of renewables in the power system.

Note that under different energy pricing policy and/or binding constraints on the CO_2 emission levels, the results could lead to a greater displacement of lignite-fired power generation plants. Not surprisingly, the tighter the CO_2 emissions cap, the higher the penetration of low carbon power generation technologies.

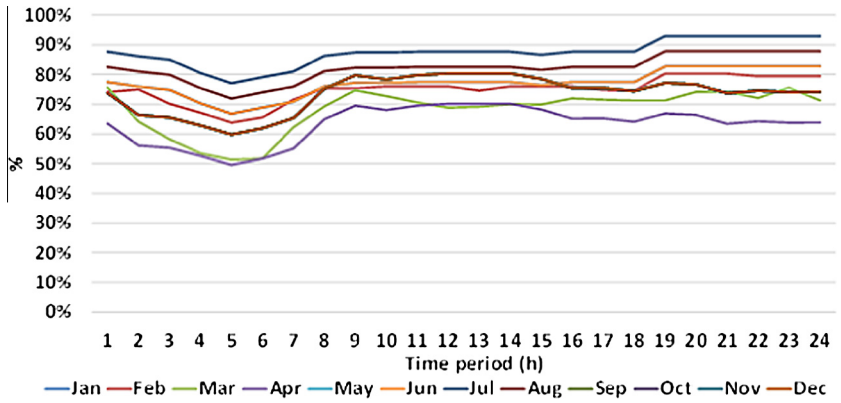

Fig. 12. Maximum availability factor of the lignite-fired units in each representative day of each month.

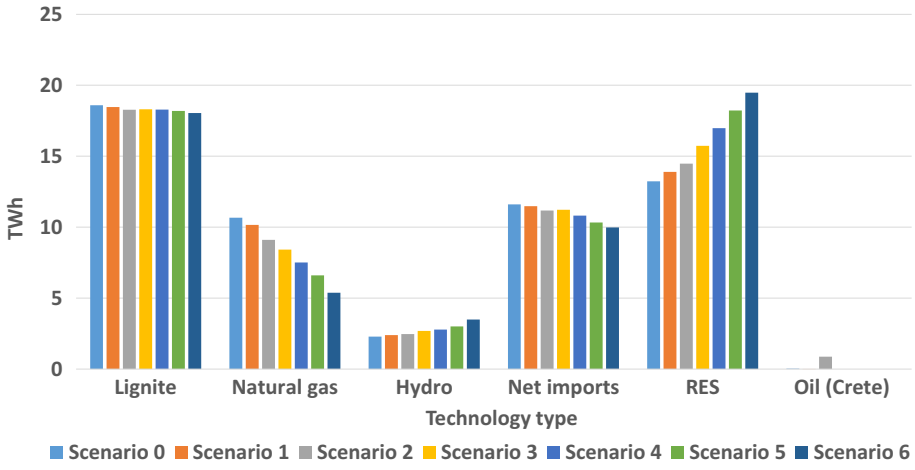

Fig. 13. Annual production mix per selected Scenario (TW h).

Hydroelectric generation is in line with the increase of the share of renewables in the power generation mix on the grounds that its contribution begins from 2.3 TW h in Scenario 0, rises to 2.7 TW h in Scenario 3, and finally reaches 3.5 TW h in Scenario 6, i.e., an increase of 52% between Scenario 0 and 6.

Net electricity imports (imports minus exports) report a slight decrease in their injections, from 11.6 TW h in Scenario 0 to 10 TW h in Scenario 6, i.e., a fall of 14%. The increasing share of the installed capacity of renewables from Scenario 0 to Scenario 6 is clearly highlighted in the amount of their power production, being equal to 13.2 TW h in Scenario 0, amounting to 15.7 TW h in Scenario 3, and finally reaching 19.5 TW h in Scenario 6, i.e., a rise of 47% between Scenario 0 and 6.

Oil-fired power generation, from units installed in Crete, is negligible in all the examined scenarios except Scenario 2, as explained in Section 5.2.

5.2. Electricity interconnection between Crete and the interconnected power system

One of the most critical decision variables determined by the mathematical model is that of the construction or not of the electricity interconnection between Crete and the interconnected power system as well as its rated capacity (in case of construction), as depicted in Fig. 14.

The results highlight that an interconnection cable with a capacity of 323.2 MW is to be constructed in Scenario 0, while the electricity flow is directed from the South subsystem (interconnected power system-mainland) to Crete. The direction of that flow explains the reason why natural gas-fired power generation remains at high levels in Scenario 0, contributing partly to Crete's demand satisfaction. Note that Scenario 0 is the scenario where the installed capacity of renewables in Crete amounts to zero.

In Scenario 1 where the renewables' installed capacity in Crete equals 272.6 MW, an interconnection cable with a capacity of 250 MW is required, while the electricity flow continues to have the same direction with that of Scenario 0, i.e., from the mainland to Crete. The reduced capacity of the electricity interconnection of Scenario 1 in comparison with that of Scenario 0, can be explained by the increased renewables' installed capacity in Crete (in Scenario 1). Electricity flows during representative days of June and November in Scenarios 0 and 1 are portrayed in Fig. 15.

In Scenario 2 where the renewables' installed capacity in Crete amounts to 500 MW, no electricity interconnection is to be installed on the grounds that the model determines that the combination of oil-fired units with the renewable power technologies (all installed in Crete) can optimally satisfy the island's power load.

A major diversification in the operation of the power system is observed in Scenarios 3–6, since the electricity flow changes its direction and it is directed from Crete to the interconnected power system. Not surprisingly, an electricity interconnection is constructed in all these scenarios, having a capacity of 267.1 MW in Scenario 3, of 569 MW in Scenario 4, of 871 MW in Scenario 5, and exceeding that of 1 GW (1177.5 MW) in Scenario 6. The main reason for that change in the electricity flow direction is the signif-

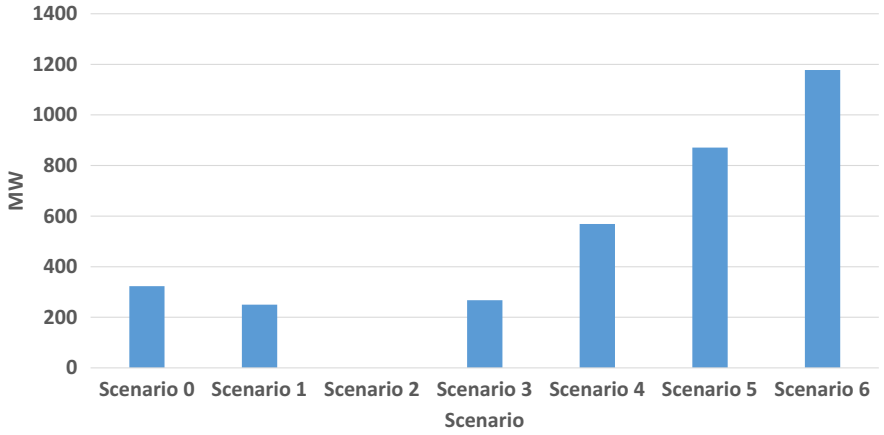

Fig. 14. Optimal capacity of the electricity interconnection between Crete and mainland (MW).

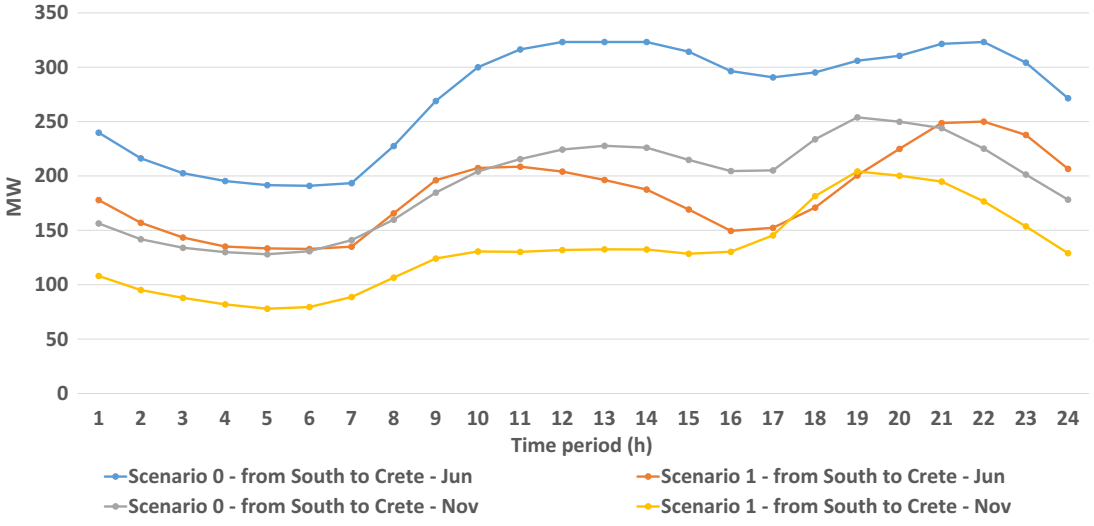

Fig. 15. Electricity flows during representative days of June and November in Scenarios 0 and 1 (MW).

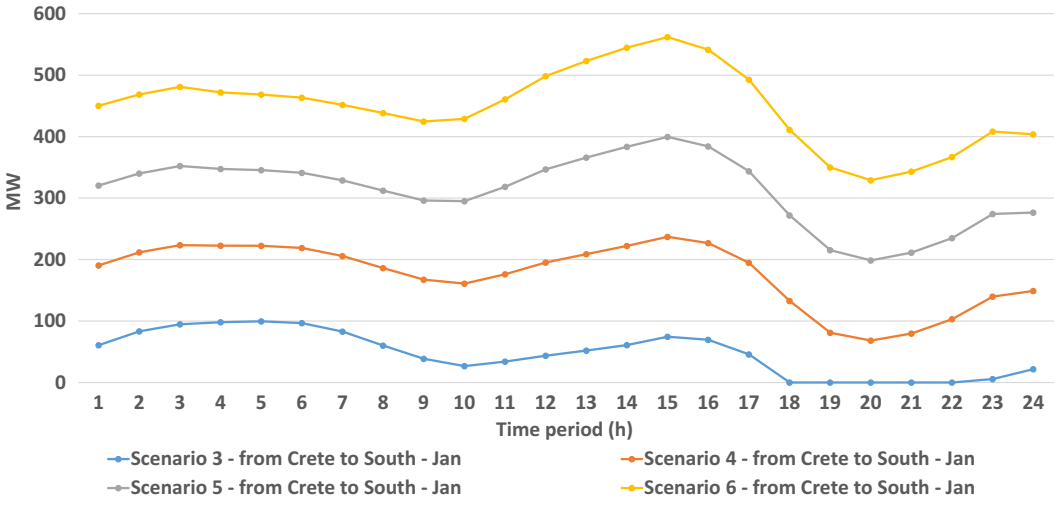

Fig. 16. Electricity flows during a representative day of January in Scenarios 3–6 (MW).

icant amount of renewables' installed capacity in Crete, being more than adequate to cover the island's power demand and as a result, the excess of electricity generation is to be exported to the mainland. Fig. 16 highlights the electricity flows determined by the mathematical model during a representative day of January for Scenarios 3–6 (MW).

5.3. System's marginal price

System's marginal price is defined as "the price that all electricity suppliers (e.g., producers, importers) are going to be paid and all power load representatives (e.g., exporters, large consumers) are going to pay" [23].

Table 4 makes a synopsis of the marginal prices (weighted average values at an annual level) observed in each subsystem, i.e., in the North, the South, and the subsystem of Crete. Note that small differences observed in Scenarios 3–6 between Crete's subsystem and the other subsystems (North and South) can be attributed to transmission line congestions (transmission limits are bounded) during some hours of the examined period.

The fact that the marginal prices of the interconnected system and the subsystem of Crete differ in Scenarios 0–2 to a significant extent can be explained by the following: (i) in Scenarios 0 and 1, oil-fired power plants, having a marginal (variable) cost of 150 €/MW h, comprise the marginal units during a number of hours of the studied period, especially during July and August when the power load is relevant high (more hours in Scenario 0 than in Scenario 1 and thus, the island's marginal price is higher in Scenario 0 than the corresponding of Scenario 1), (ii) in the absence of an electricity interconnection between Crete and mainland in Scenario 2, oil-fired units of Crete always constitute the marginal units and thus, the island's marginal price equals 150 €/MW h.

In general, a trend of gradual decrease in the values of the marginal price can be observed which is due to the significant penetration of renewables in Crete which have a zero marginal cost and they are given priority when entering the power system.

Table 4
Annual weighted average marginal price values per subsystem and scenario (€/MW h).

Scenario	North (€/MW h)	South (€/MW h)	Crete (€/MW h)
Scenario 0	44.26	44.26	58.90
Scenario 1	43.91	43.91	50.21
Scenario 2	43.19	43.19	150.00
Scenario 3	43.35	43.35	43.20
Scenario 4	42.49	42.49	42.35
Scenario 5	41.43	41.43	41.32
Scenario 6	40.49	40.49	40.35

5.4. Reserves' provision

With regards to reserves' provision, a significant variation is observed in their allocation per technology type. As described in Section 4, the penetration of renewables in Crete leads to increasing needs for secondary-up and -down, fast secondary-up and -down as well as tertiary reserves.

Fig. 17 shows the annual weighted average percentages of the secondary-up reserve provision allocation per technology type. Note that lignite units cannot provide secondary reserve. A positive correlation between the increasing share of renewables and the secondary-up reserve provision by hydroelectric units is high-

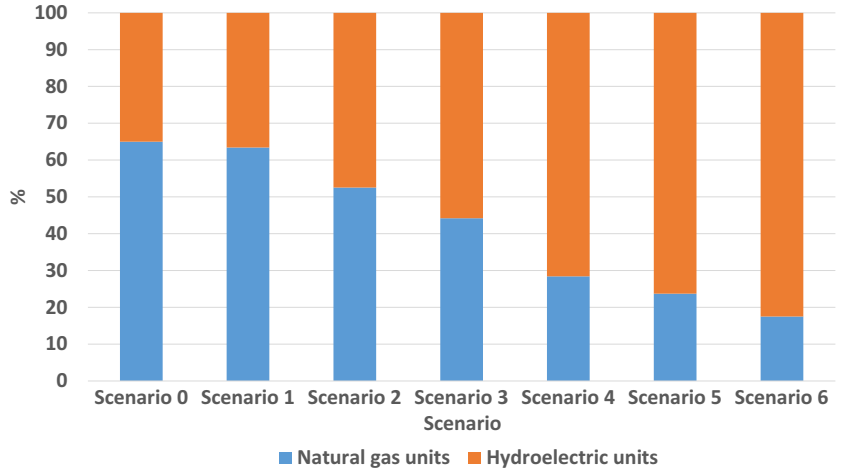

Fig. 17. Annual weighted average percentages of the secondary-up reserve provision allocation per technology type (%).

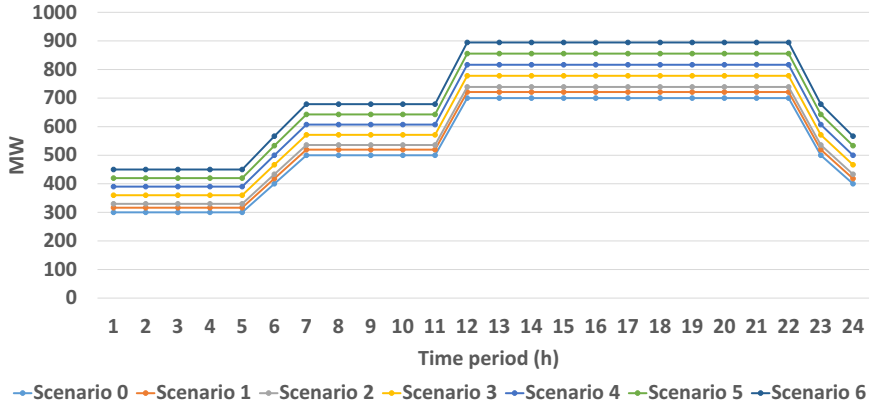

Fig. 18. Secondary-up reserve requirements per day at an hourly level (the same during all months) in all scenarios (MW).

lighted since the share of hydro units to the total secondary-up reserve provision of each scenario starts from 35% of the total in Scenario 0, rises to 55.8% in Scenario 3, and reaches the high 82.5% in Scenario 6. Fig. 18 shows the secondary-up reserve requirements per day at an hourly level (the same during all months) in all scenarios.

On the other hand, natural gas units are determined to reduce their share in that reserve type provision from 65% of the total in Scenario 0 to the low 17.5% in Scenario 6. The fact that natural gas units lose their economic competitiveness in relation to lignite units combined with the significant penetration of renewables prevents them from contributing to reserve provision to a significant extent. Note that a power unit can provide secondary reserve only if it remains dispatchable during that period.

A similar trend is also observed in the secondary-down reserve provision allocation per technology type, where hydro units enhance their contribution since their share more than doubles between Scenarios 0 and 6 in percentage terms (even higher in absolute terms). Conversely, natural gas units lose their share, albeit at a less intense rate than the corresponding in the secondary-up reserve type (see Fig. 19).

Another aspect that reveals the strategic value of hydroelectric units and the flexibility they provide to the system when there is abundance of renewables is the allocation mix of the fast secondary-up and -down reserve types. Fast secondary-up and -down reserve types refer to that secondary-up and -down reserve type required by the system within a time period of 1 min. Even in the absence of renewables in Crete (but with the existence of those in the interconnected power system), their share equals 69% of the total in the fast secondary-up and 55% of the total in the fast secondary-down reserve type (Scenario 0). As there is gradual installation of more renewables in Crete (from Scenario 1 to 6), the corresponding percentages amount to 81.5% (up) and 70.6% (down) in Scenario 2, rise to 89.7% (up) and 87.1% (down) in Scenario 4, and finally reach 93.7% (up) and 93.8% (down) in Scenario 6. All the above are summarized in Fig. 20.

5.5. CO_2 emissions

When it comes to the evolution of the CO_2 emissions at a yearly level, these share similar values in the first three scenarios of the study (Scenarios 0–2). More specifically, the amount of the CO_2 emissions released in the atmosphere from the thermal power units equals 30.4 Mt in Scenario 0, 29.9 Mt in Scenario 1, and 30.2 Mt in Scenario 2. The difference between the CO_2 emissions of Scenarios 0 and 1 can be attributed to the increase in the RES

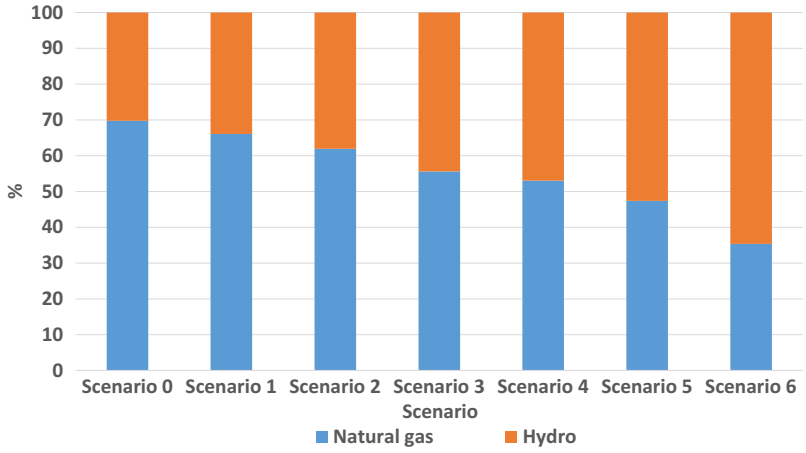

Fig. 19. Annual weighted average percentages of the secondary-down reserve provision allocation per technology type (%).

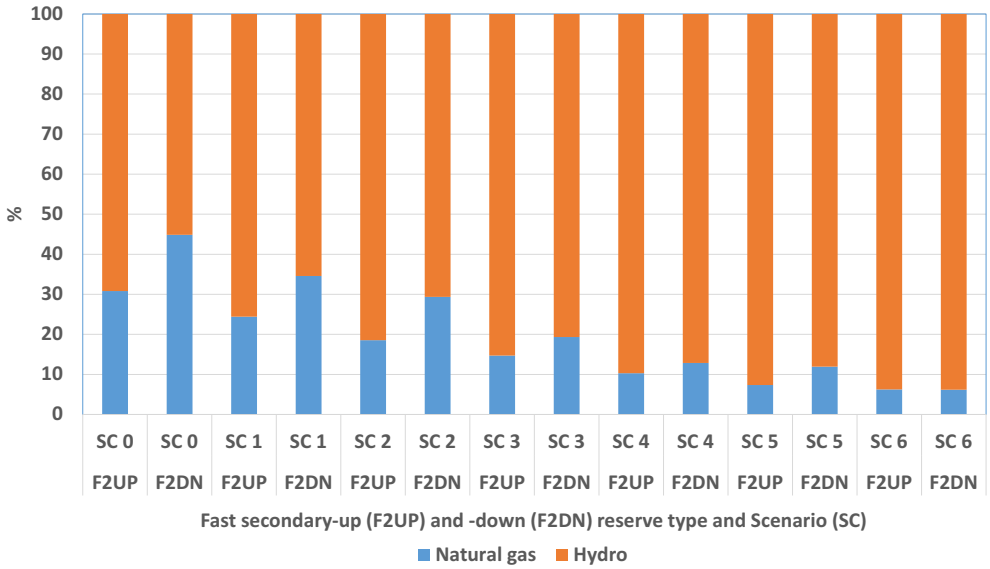

Fig. 20. Fast secondary-up and -down reserve allocation per technology type and scenario (%).

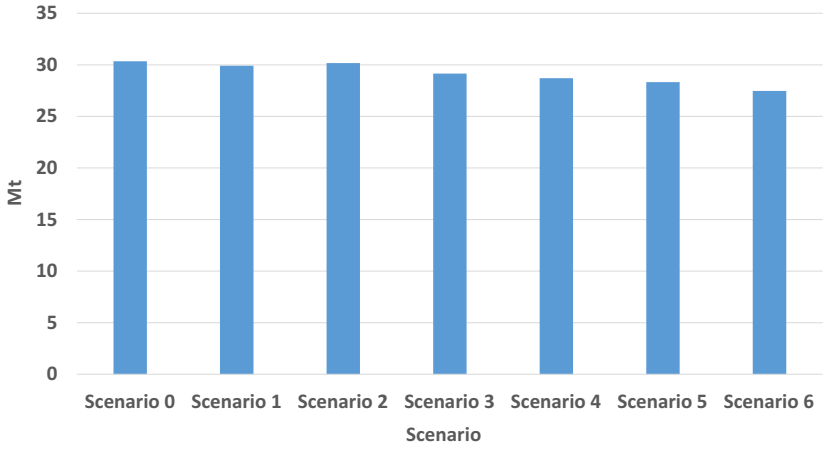

Fig. 21. CO_2 emission evolution in each selected scenario (Mt).

capacity due to the interconnection with the island of Crete, while the small increase in the amount of CO_2 emissions of Scenario 2 – when compared to that of Scenario 1 – is due to the fact that a portion of Crete's load is met by the existing oil-fired units of the island, since no interconnection is determined by the model.

The fact that an interconnector is to be installed in the remaining scenarios (Scenarios 3–6) along with the gradual increase in the RES installed capacity of Crete, leads to a subsequent decrease in the amount of the CO_2 emissions. Indeed, these amount to 29.2 Mt in Scenario 3 (a drop of 3.9% in comparison with those of Scenario 0), 28.7 Mt in Scenario 4 (a decrease of 5.4% in comparison with those of Scenario 0), 28.3 Mt in Scenario 5 (a decline of 6.7% in comparison with those of Scenario 0), and 27.5 Mt in Scenario 6 (a reduction of 9.5% in comparison with those of Scenario 0). All these are reflected in Fig. 21. Note that a mandatory CO_2 mitigation target is not incorporated in the mathematical model and the results provided represent the real operation of the power markets. The impacts on CO_2 emissions would be significant should the natural gas combined cycle gas turbines become more competitive in economic terms than the lignite-fired units, considering that their emission factor is about 0.4 tCO_2/MW h compared to 1.1–1.6 tCO_2/MW h for the lignite units operating in Greece.

6. Concluding remarks

A generic Mid-term Energy Planning (MEP) problem is integrated with a Unit Commitment (UC) model to provide optimal solutions regarding the annual energy balance and the feasibility of the interconnection of an autonomous power system with the interconnected one.

A real-life case study, concerning the potential interconnection of the Crete Island with the mainland power system, is used to illustrated the applicability of the proposed model. Various scenarios have been considered, showing the effect on the system marginal price, and also illustrating if there is a difference among the different zones in Greece, which in practice shows that there is a bottleneck and requires re-dimensioning of the interconnectors. The results provides indication on the evolution of the weighted average System Marginal Price at the different zones in Greece, namely the North Zone, the South Zone and the Crete Island, for the different scenarios of the penetration of renewables (wind and photovoltaics) in the Crete Island and the size of the DC Interconnector of the mainland electric system with the system of Crete.

The results highlight that lignite (being a domestic fuel in Greece) units comprise the most economical fossil-fuel power generation technology based on the assumptions we considered for the fuel and CO_2 emission allowances costs, and thus the model determines their higher utilization than that of the natural gas combined cycle gas turbine units (according to the data employed in that case). Not surprisingly, natural gas price is characterized by high volatility (correlated in part with that of oil) and this situation can be diversified changing the units' economic merit order. All in all, the economic competitiveness of each technology continues to be the most critical factor in the operation/dispatch of a power generation unit. It goes without saying that under different cost and other technological data, as well as under tighter regulations in terms of CO_2 emissions, the optimal power generation mixture will alter.

Furthermore the results indicate the benefits and the services provided by the hydroelectric units, while the gradually increasing share of renewables in Crete exerts downward pressure on the system's marginal price and on the share of natural gas-fired units in the power generation mix. The renewables' capacity in Crete, according to the selected scenario, constitutes the key driver for the construction (or not) of the DC interconnector as well as for its rated (nominal) capacity. According to the amount of the installed capacity of renewables, Crete can be a net power importer or can be converted into a net electricity exporter, contributing also to the CO_2 emissions mitigation.

The model also allows an examination of extensive scenarios, examining different evolution of critical values of natural gas price, CO_2 price, renewables' investment cost, DC interconnector cost etc. Moreover, it enables the assessment of the investment decision on critical transmission system elements, such as the DC cable, by estimating its pay-back period is about 3–7 years, depending on the oil price, the cost of financing, the Weighted Average Cost of Capital and any technical constraints imposed by the Transmission System Operator.

The proposed integrated model incorporates all the critical features for providing a robust decision making tool, that would be very useful to real problems for the Transmission System Operator. The detailed incorporation of actual values for the above mentioned variables will allow the actual quantification on the break-even point that identifies the size of the cable and the penetration of renewables. This will be even more robust, if actual values for supplementary regulated costs are considered, such as network costs, social welfare costs and special tax for emissions reduction (ETMEAR), but as well the actual levelized cost of energy of the wind and solar plants depending on the installed capacity.

A further extension of the model is to tackle the needs for flexibility, depending on the penetration level of the renewables. This

will provide a clear price signal on the flexible capacity needed. Furthermore, the incorporation of this cost in the overall energy system cost will provide a better treatment of the renewables, as it will practically increase the levelized cost of electricity and competitiveness of the renewables compared to other technologies.

References

[1] International Energy Agency (IEA). Seamless power markets: regional integration of electricity markets in IEA member countries. Paris: OECD/IEA; 2014. Available online at:Available from: <https://www.iea.org/publications/freepublications/publication/SEAMLESSPOWERMARKETS.pdf> [last accessed 21.11.15].

[2] International Energy Agency (IEA). Energy and climate change - world energy outlook special report. Paris: OECD/IEA; 2015. Available online at:Available from: <https://www.iea.org/publications/freepublications/publication/WEO2015SpecialReportonEnergyandClimateChange.pdf> [last accessed 21.11.15].

[3] Fürsch M, Hagspiel S, Jägemann C, Nagl S, Lindenberger D, Tröster E. The role of grid extensions in a cost-efficient transformation of the European electricity system until 2050. Appl Energy 2013;104:642–52.

[4] Purvins A, Zubaryeva A, Llorente M, Tzimas E, Mercier A. Challenges and options for a large wind power uptake by the European electricity system. Appl Energy 2011;88:1461–9.

[5] Van den Bergh K, Couckuyt D, Delarue E, D'haeseleer W. Redispatching in an interconnected electricity system with high renewables penetration. Electric Power Syst Res 2015;127:64–72.

[6] Pineau PO, Dupuis DJ, Cenesizoglu T. Assessing the value of power interconnections under climate and natural gas price risks. Energy 2015;82:128–37.

[7] Lienert M, Lochner S. The importance of market interdependencies in modeling energy systems – the case of the European electricity generation market. Int J Electr Power Energy Syst 2012;34:99–113.

[8] Tande JOG, Korpås M. Impact of offshore wind power on system adequacy in a regional hydro-based power system with weak interconnections. Energy Proc 2012;24:131–42.

[9] Lynch MÁ, Tol RSJ, O'Malley MJ. Optimal interconnection and renewable targets for north-west Europe. Energy Policy 2012;51:605–17.

[10] Denny E, Tuohy A, Meibom P, Keane A, Flynn D, Mullane A, et al. The impact of increased interconnection on electricity systems with large penetrations of wind generation: a case study of Ireland and Great Britain. Energy Policy 2010;38:6946–54.

[11] Edmunds RK, Cockerill TT, Foxon TJ, Ingham DB, Pourkashanian M. Technical benefits of energy storage and electricity interconnections in future British power systems. Energy 2014;70:577–87.

[12] Chang Y, Li Y. Power generation and cross-border grid planning for the integrated ASEAN electricity market: a dynamic linear programming model. Energy Strategy Rev 2013;2:153–60.

[13] Zafeiratou E, Spataru C. Investigation of high renewable energy penetration in the island of Syros following the interconnection with the national grid system. Energy Proc 2015;83:237–47.

[14] Magnago FH, Alemany J, Lin J. Impact of demand response resources on unit commitment and dispatch in a day-ahead electricity market. Int J Electr Power Energy Syst 2015;68:142–9.

[15] Simoglou CK, Bakirtzis EA, Biskas PN, Bakirtzis AG. Optimal operation of insular electricity grids under high RES penetration. Renewable Energy 2016;86:1308–16.

[16] Vidal-Amaro JJ, Østergaard PA, Sheinbaum-Pardo C. Optimal energy mix for transitioning from fossil fuels to renewable energy sources – the case of the Mexican electricity system. Appl Energy 2015;150:80–96.

[17] Pereira S, Ferreira P, Vaz AIF. Optimization modeling to support renewables integration in power systems. Renew Sustain Energy Rev 2016;55:316–25.

[18] Forrest S, MacGill I. Assessing the impact of wind generation on wholesale prices and generator dispatch in the Australian National Electricity Market. Energy Policy 2013;59:120–32.

[19] Clò S, Cataldi A, Zoppoli P. The merit-order effect in the Italian power market: the impact of solar and wind generation on national wholesale electricity prices. Energy Policy 2015;77:79–88.

[20] Clancy JM, Gaffney F, Deane JP, Curtis J, Ó Gallachóir BP. Fossil fuel and CO_2 emissions savings on a high renewable electricity system – a single year case study for Ireland. Energy Policy 2015;83:151–64.

[21] Zafirakis D, Chalvatzis KJ, Baiocchi G. Embodied CO_2 emissions and cross-border electricity trade in Europe: rebalancing burden sharing with energy storage. Appl Energy 2015;143:283–300.

[22] Hellenic Independent Power Transmission System Operator S.A. (ADMIE). Available online at: <http://www.admie.gr/> [last accessed 21.01.16].

[23] Koltsaklis NE, Georgiadis MC. A multi-period, multi-regional generation expansion planning model incorporating unit commitment constraints. Appl Energy 2015;158:310–31.

[24] Koltsaklis NE, Dagoumas AS, Kopanos GM, Pistikopoulos EN, Georgiadis MC. A spatial multi-period long-term energy planning model: a case study of the Greek power system. Appl Energy 2014;115:456–82.

[25] Koltsaklis NE, Liu P, Georgiadis MC. An integrated stochastic multi-regional long-term energy planning model incorporating autonomous power systems and demand response. Energy 2015;82:865–88.

[26] Hellenic Independent Power Transmission Operator (ADMIE). Study for the development of the power system of Crete. Athens: ADMIE; 2011. Available online at:Available from: <http://www.admie.gr/fileadmin/user_upload/Files/study/MELETI_DIASYNDESIS_TIS_KRITIS_EKTENIS_PERILIPSI.pdf> [last accessed 21.11.15].

[27] Hellenic Electricity Distribution Network Operator S.A. (HEDNO). Monthly reports of RES & thermal units in the non-interconnected islands, 2014. Athens: HEDNO; 2014. Available online at:Available from: <http://www.deddie.gr/Documents2/Fotovolt...> [last accessed 21.01.16].

[28] Hellenic Electricity Distribution Network Operator S.A. (HEDNO). Monthly reports of RES & thermal units in the non-interconnected islands, 2015. Athens: HEDNO; 2015. Available online at:Available from: <http://www.deddie.gr/Documents2/MDN/PLI...> [last accessed 21.01.16].

[29] Morales JM, Conejo AJ, Madsen H, Pinson P, Zugno M. Integrating renewables in electricity markets. International series in operations research & management science, vol. 205. Springer Publications; 2014.

[30] GAMS Development Corporation. GAMS – a user's guide. Washington, DC; January 2016. http://www.gams.com/help/topic/gams.doc/userguides/GAMSUsersGuide.pdf> [last accessed 21.01.16].